Contribution of the eye and of *opn4xa* function to circadian photoentrainment in the diurnal zebrafish

Clair Chaigne[1], Dora Sapède[1,2] Xavier Cousin[3], Laurent Sanchou[4], Patrick Blader[1] and Elise Cau[1*]

[1] Unité de Biologie Moléculaire, Cellulaire et du Développement (MCD, UMR5077) Centre de Biologie Intégrative (CBI, FR 3743), Université de Toulouse 3/UPS, CNRS, UPS, France

[2] IRMB, Université de Montpellier, INSERM, Montpellier, France.

[3] MARBEC, Université de Montpellier, CNRS, Ifremer, IRD, INRAE, Route de Maguelone, F-34250 Palavas, France.

[4] Centre de Biologie Intégrative (CBI, FR 3743), Université de Toulouse 3/UPS, CNRS, UPS, France

[*]Corresponding author: elise.cau@univ-tlse3.fr

Classification: Biological Sciences. Neurosciences.

Contributions: CC: performed research, analyzed data, wrote the paper. DS, XC, LS, PB: contributed new reagents/analytic tools, EC: designed research, performed research, analyzed data, wrote the paper, contributed new reagents/analytic tools.

Abstract: The eye is instrumental for controlling circadian rhythms in mice and human. Here, we address the conservation of this function in the zebrafish, a diurnal vertebrate. Using *lakritz (lak)* mutant larvae, which lack retinal ganglion cells (RGCs), we show that while a functional eye contributes to masking, it is largely dispensable for the establishment of circadian rhythms of locomotor activity. Furthermore, the eye is dispensable for the induction of a phase delay following a pulse of white light at CT 16 but contributes to the induction of a phase advance upon a pulse of white light at CT21. Melanopsin photopigments are important mediators of photoentrainment, as shown in nocturnal mammals. One of the zebrafish melanopsin genes, *opn4xa*, is expressed in RGCs but also in photosensitive projection neurons in the pineal gland. Pineal *opn4xa*+ projection neurons function in a LIGHT ON manner in contrast to other projection neurons which function in a LIGHT OFF mode. We generated an *opn4xa* mutant in which the pineal LIGHT ON response is impaired. This mutation has no effect on masking and circadian rhythms of locomotor activity, or for the induction of phase shifts, but slightly modifies period length when larvae are subjected to constant light. Finally, analysis of *opn4xa;lak* double mutant larvae did not reveal redundancy between the function of the eye and *opn4xa* in the pineal for the control of phase shifts after light pulses. Our results support the idea that the eye is not the sole mediator of light influences on circadian rhythms of

locomotor activity and highlight differences in the circadian system and photoentrainment of behaviour between different animal models.

Author summary: Experiments performed in mice have established a crucial role for the eye in general and melanopsin expressing cells in particular in the control of circadian rhythms most notably during photoentrainment, by which circadian rhythms adapt to a changing light environment. In marked contrast to this, we show that in zebrafish the eye and photosensitivity dependent on one of the melanopsin genes, *opn4xa*, which is expressed in both the eye and the pineal gland, are largely dispensable for correct circadian rhythms. These results provide insight that the light sensors orchestrating circadian rhythms of locomotor activity are different between animal models supporting that vertebrates might employ different molecular/cellular circuits for photoentrainment of behaviour depending on their phylogeny and/or temporal niche.

INTRODUCTION

Light has a profound influence on the physiology and behaviour of living organisms. In particular, it controls circadian rhythms that in turn regulate a variety of biological functions. Circadian rhythms are defined by their period of approximately 24 hours. Once established, these rhythms persist in constant conditions, which has fostered the concept of an endogenous time-keeping mechanism known as the circadian system. Nonetheless, external cues are required to synchronize (or 'entrain') circadian rhythms with the exogenous environmental conditions. For instance, light entrains the circadian system through a process referred to as photoentrainment (see (Bhadra et al., 2017) for a review).

In mouse, photoentrainment depends on a functional retina. Eye enucleated mice or mice lacking retinal ganglion cells (RGCs) do not entrain to LD (Light/Dark) cycles and thus behave as if they were in constant darkness (Brzezinski et al., 2005; Freedman et al., 1999; Wee et al., 2002). Similarly, in human, fifty percent of blind people exhibit circadian misalignment with the LD cycles (Hartley et al., 2018; Lockley et al., 2007; Sack et al., 1992). In mouse, photoentrainment depends on a specific subtype of RGCs expressing the photopigment melanopsin, which is encoded by the *Opn4* gene. These RGCs are sensitive to blue light and are referred to as ipRGCs for "intrinsically photosensitive RGCs". Mice mutant for *Opn4* shows a diminished phase-delay in response to a pulse of light administered at circadian time 16 (CT 16; at the beginning of the subjective night) but entrain normally to LD cycles (Panda et al., 2002; Ruby et al., 2002). In contrast, mice with no ipRGCs or with impaired neurotransmission from ipRGCs show no entrainment to LD as well as no phase delay

following a light pulse at CT16 (Gompf et al., 2015; Güler et al., 2008; Kofuji et al., 2016). The difference between the phenotypes observed when only melanopsin photosensitivity is impaired compared to the models where ipRGCs inputs to the brain are lost is thought to result from the influence of classical rods and cone photoreceptors on ipRGCs. Indeed, both rods and cones have been shown to play a role during photoentrainment and to signal to ipRGCs (Altimus et al., 2008; Belenky et al., 2003; Calligaro et al., 2019; Dkhissi-Benyahya et al., 2007; Dollet et al., 2010; Perez-Leon et al., 2006; Wong et al., 2007). Thus, ipRGCs function as a hub that integrates and transmits light information to the brain through a direct projection to the core of the suprachiasmatic nucleus (SCN; (Baver et al., 2008; Fernandez et al., 2016; Li and Schmidt, 2018)).This hypothalamic nucleus functions as a 'master clock' that synchronizes peripheral clocks present everywhere in the body.

In addition to photoentrainment, ipRGCs also control the increase of period length when animals are placed in constant light (LL) (Panda et al., 2002; Ruby et al., 2002) and are required for a process of maturation of the circadian clock that sets the definitive period of locomotor rhythms in LD and in constant darkness (DD, Chew et al., 2017). Finally, in addition to their crucial influence on the circadian system, murine ipRGCs also control masking, a direct suppressive effect of light on locomotor activity. This activity is thought to involve different ipRGC subtypes than the ones that impact the circadian system (Rupp et al., 2019).

ipRGCs are well established to mediate circadian and direct effects of light on behaviour in nocturnal mammals. Based on the conservation of the nervous system, observations made in human blind people and the description of ipRGC populations in the diurnal rodent Arvicanthis ansorgei as well as in human, ipRGCs are considered to play a similar role in diurnal mammals (Karnas et al., 2013; Mure, 2021). While the zebrafish has emerged as a powerful non-mammalian diurnal vertebrate model for chronobiology, the neural circuit controlling photoentrainment of behaviours has not been identified in this species. The observation that two species of cavefishes bearing eye degeneration : *Astyanax mexicanus* and *Phreatichthys andruzzii* do not show robust light-entrainable circadian locomotor activity rhythms could suggest that eye function is crucial for photoentrainment of locomotor rhythms in fishes (Cavallari et al., 2011). However, the observed circadian locomotor phenotypes could result from additional photoreceptive deficits. Indeed, *Phreatichthys andruzzii* present mutations in several opsin genes that are expressed in extra-ocular locations (Cavallari et al.. 2011). While the function of the eye regarding circadian rhythms of behaviours has not been addressed in fishes, in the zebrafish model, an additional level of complexity arises from the observation that all cell types are photosensitive (Carr and Whitmore, 2005; Vallone et al., 2004; Whitmore et al., 2000) . This local photodetection could serve local functions (metabolism, transcription, cell cycle) or participate to the control of behaviors, although some level of central control is expected for orchestrating a complex process such as behavior. As such, the

101 relative importance of central versus peripheral control for the photoentrainment of locomotor
102 activity is still unclear.

103 To begin addressing how photoentrainment is controlled in zebrafish we first tested the role
104 of the retina using *lakritz* (*lak*) mutants in which all RGCs fail to develop and as such no connection
105 exist between the eye and the CNS (Kay et al., 2001). *lak* mutant larvae entrain to LD cycles and
106 maintain rhythms of locomotor activity with a period similar to their control siblings in constant
107 darkness (DD) but show subtle alterations in constant light (LL). While we detected no defect in
108 phase shifting in response to a pulse of white light produced in the early subjective night (CT16) in *lak*
109 -/- larvae, we observed a reduction of the phase shift induced upon a similar pulse of light at CT21 in
110 *lak* mutants. The zebrafish possesses five melanopsin genes that are all expressed in the retina,
111 including *opn4xa* and *opn4b* in larval RGCs (Kölsch et al., 2021; Matos-Cruz et al., 2011). In addition,
112 melanopsin expression is detected in extra-retinal tissues. For instance, *opn4xa* is expressed in a
113 subpopulation of projection neurons in the pineal gland. Interestingly these *opn4xa*+ projection
114 neurons function in a LIGHT ON fashion while *opn4xa*- projection neurons function in a LIGHT OFF
115 manner (Sapède et al., 2020). We engineered an *opn4xa* mutant in which the LIGHT ON response of
116 the pineal is impaired; *opn4xa* -/- larvae successfully entrain to LD cycles and maintain rhythms of
117 locomotor activity in constant conditions albeit with a reduction of period in LL. Pulses of white light
118 at CT16 and CT21 induced similar phase shifts in *opn4xa* mutant and *opn4xa*/*lak* double mutant
119 larvae compared to controls. Our results suggest that the function of the retina and the LIGHT ON
120 response of the pineal gland are not absolutely required for circadian photoentrainment in zebrafish,
121 thus further highlighting differences in the circadian system and circadian photoentrainment
122 between mammals and zebrafish.

123

124 **RESULTS**

125 **The zebrafish eye is dispensable for the establishment of circadian rhythms**

126 Photoentrainment in mouse and human requires a functional eye. We took advantage of *lak*
127 mutant larvae that lack RGCs to address whether this role for the eye is conserved in the diurnal
128 zebrafish. Homozygous *lak* mutant larvae lack neuronal connections between the eye and the brain
129 and do not display an optomotor response (Covello et al., 2020; Kay et al., 2001; Neuhauss et al.,
130 1999). The gene mutated in *lak*, encoding for the bHLH transcription factor ATOH7 (ATH5) is
131 expressed in the developing retina and nowhere else (Masai et al., 2000). The lak^{th241}allele we used
132 bears a point mutation functions as a null allele which result in a total absence of both RGCs and a
133 neural connection between the eye and the brain (Kay et al., 2001). We compared the locomotor
134 activity of homozygous *lak* mutants with siblings (*lak*+/+ and *lak*+/-) in different illumination

135 conditions. For each of these conditions, three independent experiments were performed. Within
136 each independent experiment, the same number of homozygous mutants and control siblings were
137 randomly selected and the mean of the three experiments was plotted. In this manner, the weight of
138 each experiment within the final mean was identical between mutant and sibling populations.

139 In cycles of 14h light: 10h dark (hereafter referred to as LD), both siblings and *lak*
140 homozygous mutant larvae exhibit rhythms of locomotor activity that are aligned with the LD cycles
141 (Fig 1B). However, compared to sibling larvae, *lak* mutants show a specific reduction of activity
142 during the day (Fig 1.B, supplemental Table 1). Sibling and *lak* mutant LD-entrained larvae placed in
143 constant darkness (DD) demonstrate rhythms of locomotor activity with similar levels (Fig 1.C,
144 supplemental Tables 2). In addition, the periods of the rhythms observed in DD did not significantly
145 differ between the two populations (Fig 1D). The reduction in activity observed during the day in LD
146 conditions thus does not affect the persistence of rhythmicity under free running conditions in DD.

147

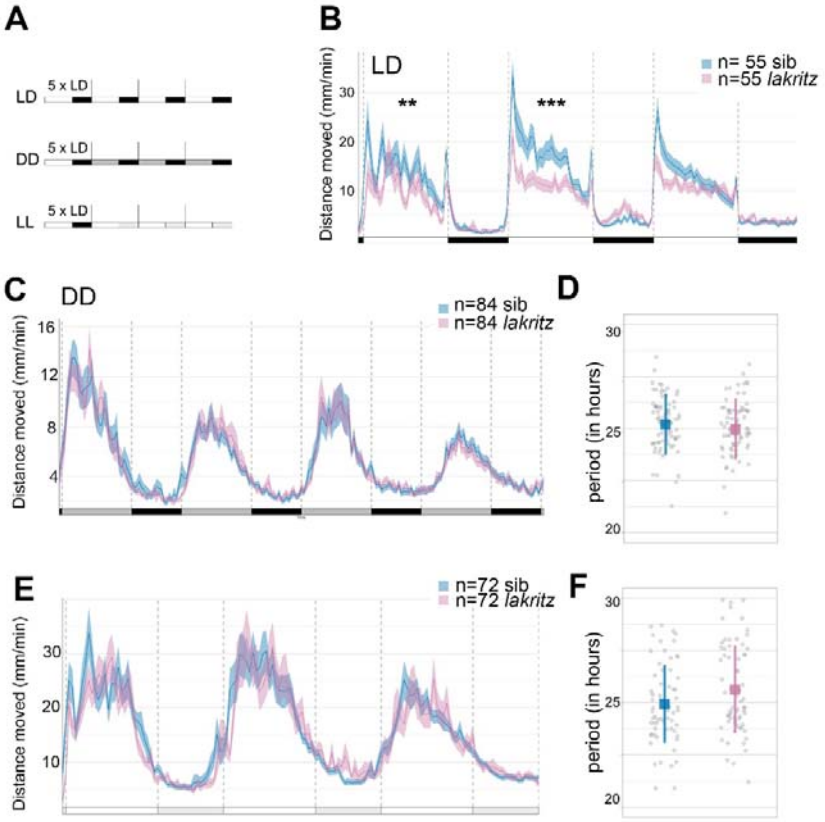

148

149 **Figure 1: Locomotor activity of larvae devoid of RGCs in LD, DD and LL**

150 **A)** Experimental design of LD, DD and LL experiments. White rectangles represent the day period,
151 while black rectangles represent the night period, light grey rectangles represent the subjective day
152 period and dark grey rectangles the subjective night. For each experiment, larvae are entrained for 5
153 LD cycles and their locomotor activity is tracked either in LD (LD), constant darkness (DD) or constant
154 light (LL) the larvae are therefore 5dpf at the beginning of locomotor activity measurements.

155 **B)** Average distance moved (mm/min) In LD. Merged data from 3 independent experiments
156 represented in 10 min bins. Error bars represent SE. The distance moved is lower in *lak* larvae than
157 control sibling larvae during the 1st (p=0.008) and 2nd days (p=0.005) but not during the 3rd day
158 (p=0.13) nor during the night (p=0.42, p=0.51 and p=0.57 for the 1st, 2nd and 3rd nights; Mann-
159 Whitney two-tailed test), see supplementary Table 1. * P<0.05, **p<0.01, ***p<0.005.

160 **C)** Average distance moved in DD. Merged data from 3 independent experiments represented in 10
161 min bins. Error bars represent SE. No differences are detected between the distance moved of
162 siblings versus *lak* larvae using a Mann-Whitney two-tailed test for each subjective night or day, see
163 supplementary Table 2.

164 **D)** Estimation of the periods using the FFT-NLLS method. Calculations were made on four complete
165 cycles in DD. The mean period is not significantly different between sibling and *lak* larvae in DD
166 (control: 25.08 ± 1.59 hours (n=114), *lak*: 24.95 ± 1.44 hours (n=83); mean ± S.D; p=0.32; Mann-
167 Whitney two-tailed test, sibling vs *lak* larvae). Each grey point represents a single larva.

168 **E)** Average distance moved in LL. Merged data from 3 independent experiments represented in 10
169 min bins. Error bars represent SE.

170 **F)** Estimation of the periods using the FFT-NLLS method. Calculations were made on three complete
171 cycles in LL. Mean± sd (in hours) is represented. Each grey point represents a larva, n= 66 siblings,
172 n=68 *lak* larvae.

173 Finally, in constant light (LL) conditions, the activity of siblings and *lak* larvae were similar.
174 The period of the *lak* mutant rhythm was slightly higher than the sibling rhythm but this difference
175 was not significant (siblings: 24.93 ± 1.87 hours (n=66), *lak*: 25.63± 2.1 hours (n=68); mean ± S.D;
176 p=0.083; Mann-Whitney). Altogether these results suggest that retinal ganglion cells and therefore a
177 neuronal connection between the eye and the brain are dispensable for the establishment of
178 circadian rhythms, their correct alignment to LD cycles and their maintenance in free running
179 conditions (DD or LL).

180 **Absence of a functional eye differentially affects the induction of a phase delay and a phase-**
181 **advance following pulses of light during the subjective night**

182 To evaluate the role for RGCs in circadian photoentrainment, we assessed the phase-shifting
183 effect of a pulse of white light on locomotor activity in *lak* larvae during the subjective night. We first
184 chose to perform such a light pulse at CT16, as this was previously shown to induce a robust phase
185 shift of the molecular clock in cell cultures (Tamai et al., 2007; Vallone et al., 2004). After entraining
186 for 5 LD cycles, larvae from *lak+/-* incrosses were further reared in DD and subjected to a pulse of
187 light during the second night in DD ("PD larvae"). Their activity was compared with the activity of

188 larvae kept in the dark for 4 days ("DD larvae"). To analyze if a phase shift was induced, we calculated
189 the difference of phase between the two last days ("after the light pulse") and the two first days
190 ("before the light pulse"), a value we refer to as "△phase" (Fig 2.A). We found that a 2-hours pulse of
191 light at CT16 induced a phase delay of locomotor activity rhythms in larvae, as the △phase of PD
192 larvae was higher than the one of DD larvae (Fig 2.B, Table 1). When the difference between the
193 Δphase of pulsed larvae minus the Δphase of larvae placed in DD was calculated, it suggests a phase
194 delay of 2.94 hours on average in PD larvae. Finally, we determined that control and *lak* mutant
195 larvae exhibit a similar phase shift in locomotor activity (Fig 2.C, Table 1) suggesting that RGCs are
196 not necessary for the circadian photoentrainment of locomotor activity to a pulse of light at the
197 beginning of the subjective night (CT16).

198

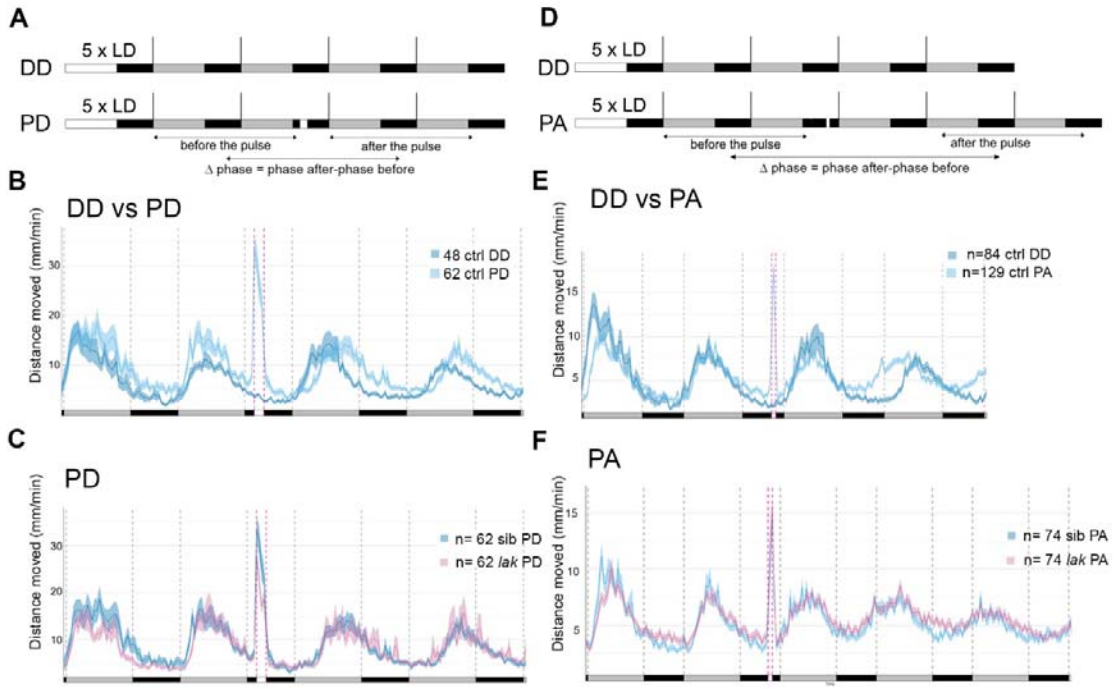

199

200 **Figure 2: Larvae devoid of RGCs still photoentrain to pulses of white light at CT16 and CT21**

201 **A)** Experimental design of phase delay (PD) experiments. White rectangles represent the day or light
202 pulse period, black rectangles represent the night period and dark grey rectangles represent the
203 subjective day. For each experiment, larvae are entrained for 5 LD cycles, the larvae are therefore
204 5dpf at the beginning of locomotor activity measurements. Locomotor activity is tracked either in
205 constant darkness for 4 days (DD) or tracked in constant darkness for 4 days and subjected to a 2-
206 hours pulse of light during the night of the 2nd day of constant darkness at CT16 (PD). The phase of
207 locomotor activity is calculated for each larva before and after the timing of the pulse for DD and PD
208 experiments and the △phase (phase after the pulse – phase before the pulse) is calculated.

B) Average distance moved by control larvae (mm/min over 10min) in DD and PD experiments. Mean ± SE. The △phase calculated using the FFT-NLLS method of PD larvae is higher than the one of DD larvae ($p<0.0001$, Mann-Whitney two-tailed test), showing that the pulse of light induced a phase delay.

C) Average distance moved merged from PD experiments represented in 10 min bins. Mean ± SE. The △phase of control versus *lak* larvae calculated using the FFT-NLLS method is not significantly different ($p=0.24$, Mann-Whitney two-tailed test). *lak* show lower levels of activity during the light pulse ($p=0.03$, Mann-Whitney two-tailed test).

D) Experimental design of phase advance (PA) experiments. The iconography is similar to A). PA-pulsed larvae were subjected to a one-hour pulse of light at CT21.

E) Average distance moved of control larvae (mm/min over 10min) in DD and PD experiments Mean ± SE. The △phase calculated using the FFT-NLLS method is negative in PA-pulsed larvae and statistically different from DD larvae ($p<0.0001$, Mann-Whitney two-tailed test), showing that the pulse of light induced a phase advance.

F) Average distance moved merged from PA experiments represented in 10 min bins. Mean ± SE.

We next performed a pulse of light at the end of the subjective night. A one hour pulse induced a phase advance that could be detected during the second circadian cycle after the pulse (Figure 2D, E). Since this phase shift is not seen during the first cycle, we analyzed larvae over an additional cycle in order to obtain enough data to perform a robust phase calculation. The difference between the Δphase of pulsed larvae (PA) minus the Δphase of larvae placed in DD alone suggests that this paradigm induced a phase advance of at least 3.7 (1.8 +1.9) hours on average. While *lak* -/- larvae showed a phase advance upon a pulse of light at CT21 (Fig 2.F, table1), this phase shift was weaker than that induced in control larvae (Δphase= -1.8 ± 7.84 for siblings versus Δphase = -0.56 ± 4.49 for *lak* -/- larvae). Although this difference in phase shift between *lak* and siblings is difficult to observe on the graph representing all the animals from the four independent experiments, it better shows when only the animals for which a phase was successfully extracted before and after the pulse (Figure 2F, Figure S1). These results suggest that a phase advance can occur in absence of RGCs although the eye contributes to photoentrainment in this context. Altogether, our results thus suggest that although phase advances and delays can occur in absence of RGCs, the absence of these cells specifically affect the response to a phase advance paradigm.

Condition	**Δphase** Mean±S.D (n)	**P value** Mann-Whitney two-tailed test
DD sib	1.9±2.56 (73)	
PD-pulsed sib	4.84±1.90 (46)	Sib : PD vs DD: ****
PD-pulsed *lak*	5.72±2.32 (37)	PD *lak* vs sib: 0.24
PA-pulsed sib	-1.83 ± 7.84 (86)	Sib: PA vs DD: ****

PA-pulsed *lak*	-0.56 ±4.49 (29)	PA *lak* vs sib: *

240

241 **Table 1: Quantification of the phase shifts in control siblings versus *lak*-/- (*lak*) larvae kept in DD or**
242 **submitted to pulses of white light at CT16 or CT21**

243 The Δphase is the difference between the phase of the two last cycles and the phase of the two first
244 cycles. A phase shift is observed in DD owing to the period that is close to 25 hours which generates a
245 ~1 hour-shift every cycle. Upon a pulse of light at CT16 or CT21 a statistical difference is observed
246 between DD and pulsed sib larvae as well as *lak* and sib larvae when the pulse of light is applied at
247 CT21 (****, p<0,0001; *, p<0,05 using a Mann-Whitney two-tailed test). For each type of paradigm,
248 (DD, PD and PA) three independent experiments were pooled.

249 To analyse a role for RGCs during masking we calculated the activity of control and *lak* larvae
250 during the pulses of light performed at CT16 and CT21. Interestingly, *lak* larvae showed a reduced
251 level of activity compared to control larvae during the pulse performed at CT16 but not at CT21
252 (CT16 : Fig 2.C, siblings: 28.33 ± 19.26 mm/min over 10min (n=62), *lak*: 21.45 ± 12.27 mm/min over
253 10min (n=51); p=0.03; Mann-Whitney two-tailed test; CT21 : Fig 2.F siblings: 16.51 ± 10.9 mm/min
254 over 10min (n=51), *lak*: 17.17 ± 7.85 mm/min over 10min (n=62); p=0.75). These results showed that
255 RGCs are involved in masking in the zebrafish larvae but in a circadian dependent manner.

256

257 ***opn4xa* function contributes to endogenous period setting in LL**

258 As circadian rhythms of locomotor activity are established and photoentrain in absence of
259 RGCs, albeit with less efficiency, we wondered if *opn4xa*+ projection neurons present in the pineal
260 gland could play a role in the establishment and photoentrainment of circadian rhythms (Sapède et
261 al., 2020). We, thus, generated a mutant allele for *opn4xa* via CRISPR/Cas9 genome editing using
262 guide RNAs targeting the second coding exon. Amongst various alleles that were generated, we
263 selected an allele that displays a 17 nucleotides insertion for further analysis (Fig 3.A). The protein
264 encoded from this allele is predicted to contain a premature stop codon (Fig S2.A) leading to a
265 truncation of the protein in the middle of the second transmembrane domain (Fig S2.B), which
266 should result in a protein devoid of a G protein interaction domain. We have verified that the two
267 alternative ORFs also generate a truncation from the mutated allele (Fig S2.C) and that the use of an
268 alternative ATG present in both the wt and the mutant allele also leads to a truncation (Fig S2. D).
269 Finally, we have used Spliceator as to verify that the mutation does not generate alternative splicing
270 sites (Spliceator (lbgi.fr)). We therefore predicted production of a null allele. Homozygous animals
271 were viable and fertile.

272 We first looked at the expression of *opn4xa* in the retina of *opn4xa*+/+ and *opn4xa* -/- larvae.
273 The RGC layer contained an average of 33 to 44 *opn4xa*+ cells (Fig S3 A-E), which number did not
274 significantly vary between the different time points suggesting an absence of diel rhythm in this

275 layer. Surprisingly, we observed a previously undescribed expression of *opn4xa* in the interneuron
276 layer with numerous cells at 4dZT0 and 5dZT0 and very few cells at the other ZT time points (Fig S3A-
277 D, F). The number of *opn4xa*+ cells in both the RGC and the interneuron layer are normal in the
278 *opn4xa* -/- retina (Fig 3B, RGC layer : *opn4xa* +/+: 26.17 ± 7.33, n= 6; *opn4xa*-/-: 23.8±6.92, n=10;
279 p=0.42 using a Mann-Whitney two-tailed test; interneurons layer : *opn4xa* +/+: 26.33± 11.5 ;
280 *opn4xa*-/-: 22.9±7.19; p=0.63 using a Mann-Whitney two-tailed test). Similarly, we have observed
281 that the number of *opn4xa* + pineal cells were similar in *opn4xa* +/+ and *opn4xa* -/- larvae (Fig 3 C,
282 *opn4xa* +/+: 4.33±1.51 n=6, *opn4xa*-/- : 4.75± 1.98 n=9, p=0.85 using a Mann-Whitney two-tailed
283 test). In addition, pineal *opn4xa*+ cells express the Wnt effector *tcf7* (Sapède et al., 2020). At 6 days
284 post fertilization, the *opn4xa*-/- pineal gland displayed normal expression of *tcf7* (*opn4xa* +/+: 5.5 ±
285 2,5 (n=4), *opn4xa-/-*: 6± 3 cells (n=3); mean ± S.D; Figure S4). Upon illumination with a 30 min pulse
286 of light, *fos* is expressed in 2-5 cells of the pineal gland (Fig 3.D). We have previously shown that this
287 expression corresponds to *opn4xa+* cells (Sapede et al., 2020). On the other hand, *fos* expression is
288 virtually absent in the pineal gland of *opn4xa-/-* embryos after a 30 min pulse of light (Fig 3.D; at 3
289 days *opn4xa* +/+: 4.8 ± 0.8 (n=9), *opn4xa-/-*: 0.25 ± 0,7 cells (n=8) per pineal; at 7 days *opn4xa* +/+:
290 5.9 ± 3,5 (n=9) *opn4xa-/-*: 0.4 ± 0,7 cells (n=13); mean ± S.D). Altogether our results suggest that
291 *opn4xa-/-* larvae contained normal numbers of *opn4xa*+ cells in the retina and the pineal gland but
292 have lost expression of *fos* following a 30 mn light pulse. We therefore used the *opn4xa* mutant as a
293 model in which the pineal ON_response is impaired.

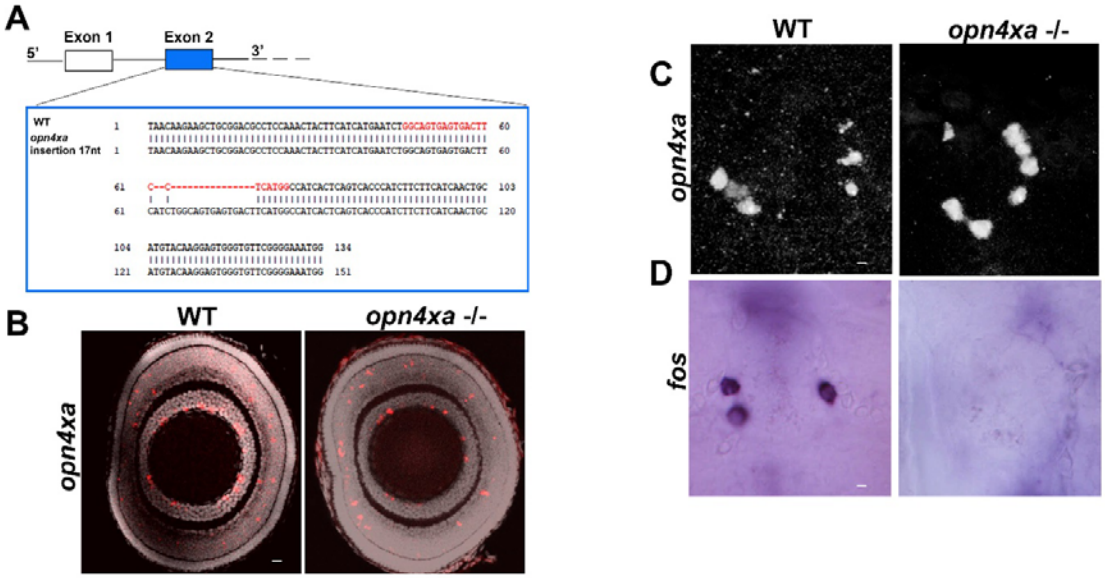

294
295 **Figure 3: Mutation in *opn4xa* abolishes light sensitivity in pineal *opn4xa+* cells** (A) Scheme showing
296 the 5' part of the *opn4xa* locus and in particular the second exon targeted by the CRISPR guide RNA
297 (target sequence is highlighted in red) as well as the WT and mutant exon2 sequences. B) In situ
298 hybridization showing *opn4xa* expression in the retina at 4 days (ZT0) (C) Expression of *opn4xa* in the

299 pineal at 4 days (ZT0) (D) *fos* expression at 3 days after 30 min of illumination. Scale bars respectively
300 represent 10 μm (B) and 5 μm (C-D).

301 To identify a role for *opn4xa* in the control of circadian rhythms, we analysed locomotor
302 behaviour of *opn4xa*-/- larvae under various illumination regimes. Similar to the analysis we
303 performed in *lak* larvae, for each of these conditions, three independent experiments were
304 performed. Within each independent experiment, the same number of *opn4xa* -/- and *opn4xa* +/+
305 siblings were randomly selected and the mean of the three experiments was plotted. We found that
306 *opn4xa* -/- larvae still entrained to LD cycles and did not show any difference in levels of locomotor
307 activity when compared to their *opn4xa* +/+ siblings (Fig 4.B + supplemental Table 4). In addition,
308 *opn4xa*-/- larvae were able to maintain rhythms of locomotor activity with a similar period as wild-
309 type larvae in DD (Fig 4.C, D). *opn4xa*-/- larvae placed in LL still showed circadian rhythms of
310 locomotor activity (Fig 4.E, F) but with several alterations. First, *opn4xa*-/- larvae were significantly
311 more active during the first night (Supplemental table 6). More importantly, in LL the period was
312 shorter for *opn4xa-/-* larvae compared to controls using both the FFT-NLLS (*opn4xa+/+:* 25.31 ± 3.29
313 hours (n=65), *opn4xa-/-:* 24.71 ± 3.32 hours (n=64); p=0.041; Mann-Whitney two-tailed test) and
314 mFourfit methods (*opn4xa+/+:* 25.84 ± 1.60 hours (n=66), *opn4xa-/-:* 25.12 ± 1.739 hours (n=66);
315 p=0.012). Altogether these results suggest that *opn4xa* contributes to endogenous period setting in
316 LL.

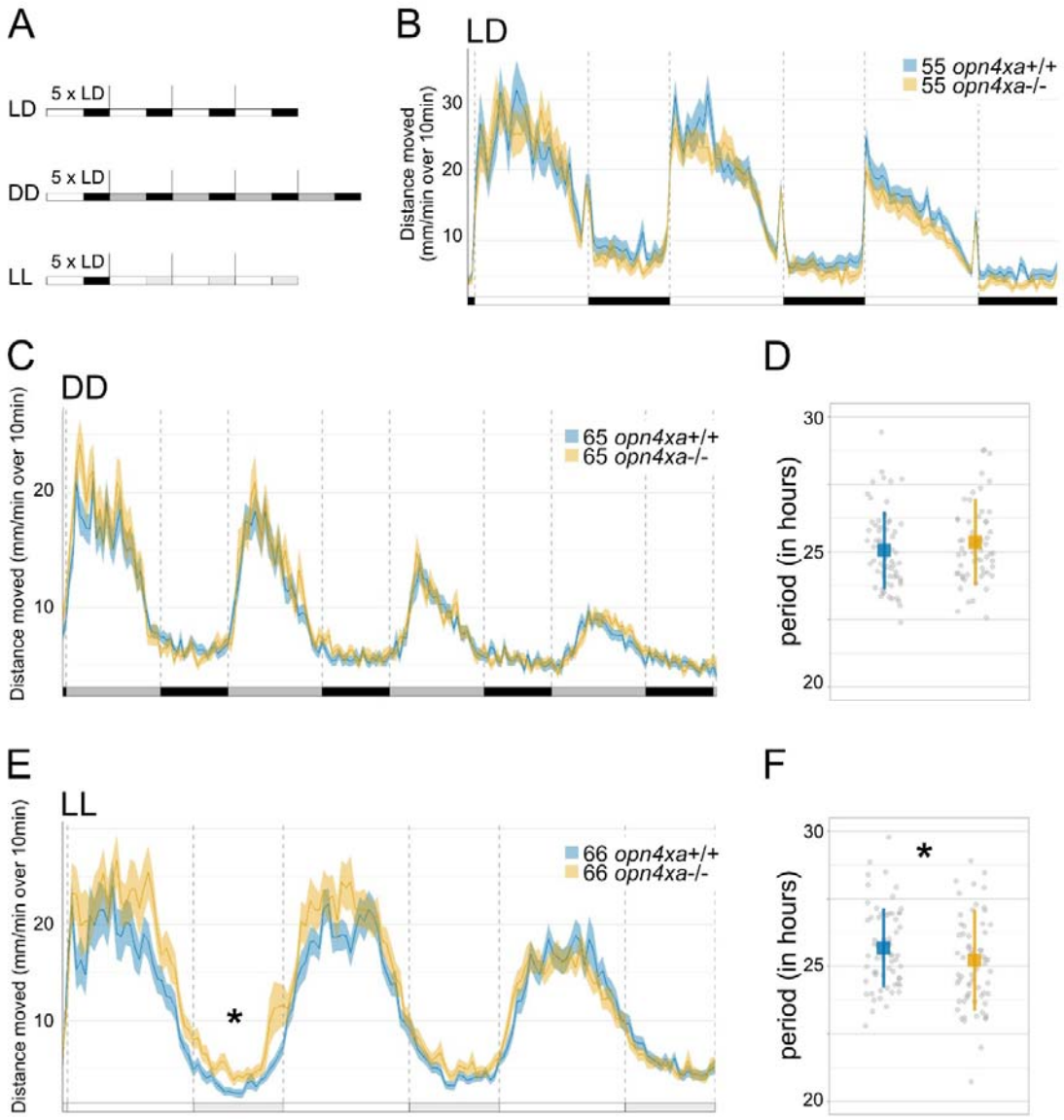

Figure 4: Locomotor activity of larvae devoid of *opn4xa*-mediated photosensitivity (*opn4xa-/-*) in LD, DD and LL

A) Experimental design of LD, DD and LL experiments. White rectangles represent the day period, black rectangles represent the night period, dark grey rectangles represent the subjective day period and light grey rectangles the subjective night. For each experiment, larvae are entrained for 5 LD cycles and their locomotor activity is tracked either in LD (LD), constant darkness (DD) or constant light (LL) the larvae are therefore 5dpf at the beginning of locomotor activity measurements.

B) Average distance moved (mm/min over 10min) of 3 independent experiments in LD. Mean ± SE. The distance moved is not different in *opn4xa+/+* and *opn4xa-/-* larvae during the 1st (p=0.73), 2nd days (p=0.50) and 3rd days (p=0.07) nor during the 1st (p=0.30), and 2nd nights (p=0.27) (supplemental Table 4). A lower level of activity is found in *opn4xa-/-* larvae during the 3rd night

330 (p=0.01) but is visually clear in only one of the 3 independent experiments (Mann-Whitney two-tailed
331 test).

332 **C)** Average distance moved (mm/min over 10min) of 3 independent experiments in DD. Mean ± SE.

333 **D)** Estimation of the periods using the FFT-NLLS method calculated over four cycles. The mean period
334 is not significantly different between control and *opn4xa*+/+ and *opn4xa-/-* larvae in DD (*opn4xa+/+:*
335 25.05 ± 1.43 hours (n=64), *opn4xa-/-:* 25.35 ± 1.60 hours (n=60); mean±SD; p=0.29; Mann-Whitney
336 two-tailed test). Mean± sd (in hours) is represented. Each grey point represents a larva.

337 **E)** Average distance moved (mm/min over 10min) of 4 independent experiments in LL. Mean ± SE.
338 *opn4xa*-/- are more active than controls during the first night (p=0.02, see supplemental Table 6).

339 **F)** Estimation of the periods using the FFT-NLLS method calculated over three cycles. The mean
340 period is significantly different between *opn4xa*+/+ and *opn4xa-/-* larvae in LL. Mean± sd (in hours) is
341 represented. Each grey point represents a larva.

342 Since *opn4xa*-/- larvae showed a slight hyperactivity during the first night as well as a subtle
343 period phenotype in LL, we began to analyse the possible molecular mechanisms behind these
344 effects using RTqPCR (Figure 5). Analysis of clock gene expression in *opn4xa*-/- versus wt background
345 reveal normal rhythms of clock genes expression in LD except for a slight increase in *tef alpha* and
346 *cry1a* in *opn4xa* -/- larvae (Figure 5 B,D). In LL after training, the expression of *bmal1a* was higher in
347 *opn4xa* -/- than in wt larvae (Figure 5A). Interestingly, the expression of some Bmal1a direct targets
348 (*cry1a*, *dec1*) was also increased (figure 5 B, C) while expression of *reverbB1, per1a, per1b, per2*
349 remain unchanged (Figure 5 E-H). Overall, only subtle and specific molecular phenotypes were
350 detected in *opn4xa* -/- larvae in LL. In addition, their relation to the locomotor activity phenotypes
351 are not clear.

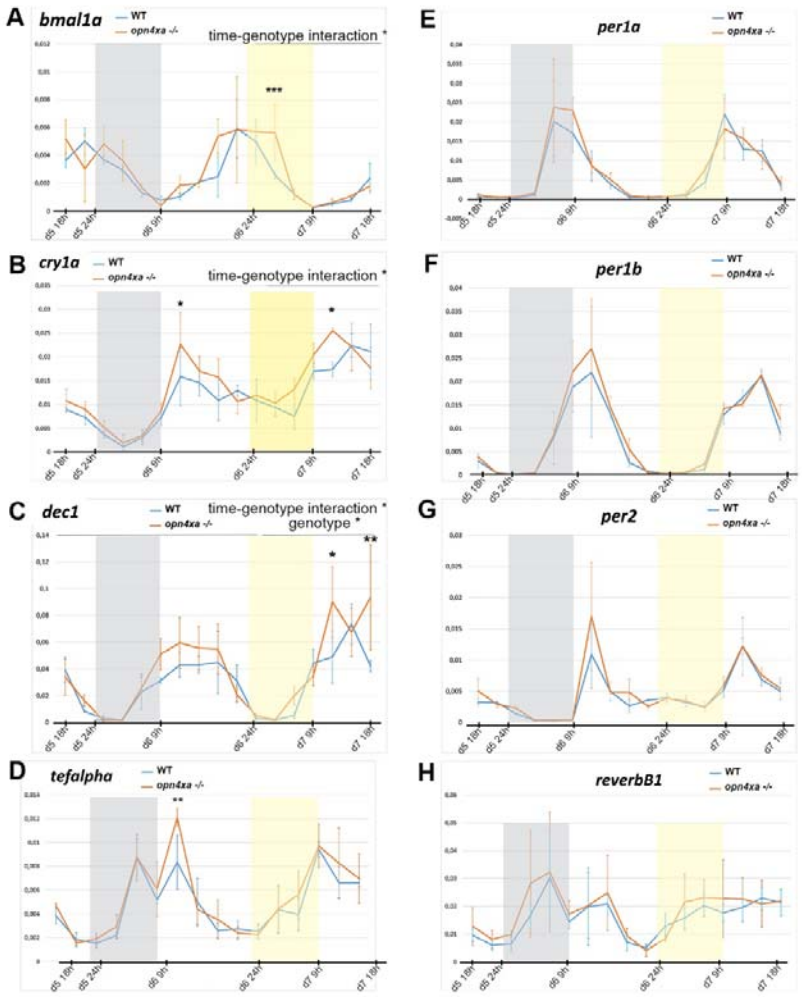

Figure 5 : *opn4xa* -/- larvae show subtle modifications of a few clock genes in LL :
RTqPCR performed on pools of 15 larvae for the gene indicated at the top of the figures. Mean expression relative to beta actin ± s.d. Three pools of larvae were used for each time point. 'wt' refers to pool of larvae from crosses of *opn4xa*+/+ animals (siblings of the *opn4xa*-/- fishes used for the *opn4xa*-/-points). Larvae were exposed to LD cycles (until d6 21h) followed by a LL cycle (from d6 21h to d7 18h). The grey rectangles represent the night phase, the yellow rectangles represent the subjective night in the LL cycle. The data were analysed using two way ANOVAs which revealed time-genotype interaction for *bmal1a* and *cry1a*, as well as statistical differences between genotypes for specific time points using Bonferroni post-hoc tests. $p< 0.05$; ** $p< 0.001$; ***$p< 0.0005$.

opn4xa function is dispensable for photoentrainment to a pulse of white light during the subjective night

We next assessed the ability of pulses of white light at CT 16 and CT21 to induce phase shifts in an *opn4xa*-/- background. We observed that under such conditions *opn4xa*-/- larvae shift their activity to the same extent as their wild-type siblings (Fig 6, Table 3). Furthermore, *opn4xa*-/- larvae

370 did not show any difference in the level of activity during the pulses of light at CT16 or CT21
371 compared to wildtype siblings, implying that photosensitivity controlled by *opn4xa* is not required for
372 masking (CT16, Fig 6.B, *opn4xa*+/+: 20.30 ± 10.03 mm/min over 10min (n=58), *opn4xa-/-*: 19.42 ±
373 10.76 mm/min over 10min (n=58); p=0.56; Mann-Whitney two-tailed test. CT21: Fig 6.D, *opn4xa*+/+:
374 12.85 ± 6.80 mm/min over 10min (n=44), *opn4xa-/-*: 16.54 ± 8.55 mm/min over 10min (n=44);
375 p=0.47). These results show that the intrinsic photosensitivity of *opn4xa* expressing cells is not
376 necessary for circadian photoentrainment or masking.

377
378

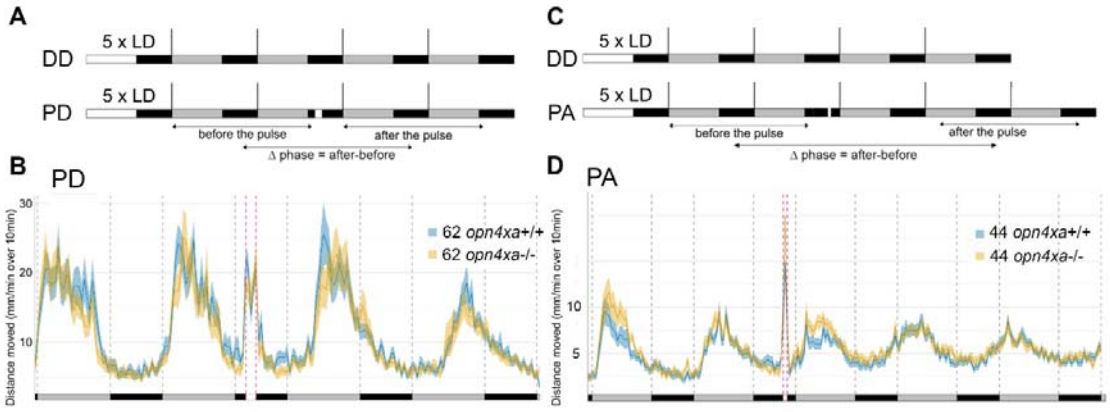

379
380 **Figure 6: Larvae devoid of *opn4xa*-mediated photosensitivity (*opn4xa-/-*) still photoentrain to**
381 **pulses of light at CT16 and CT21.**

382 **A)** Experimental design of phase shift experiments. White rectangles represent the day or light pulse
383 period, black rectangles represent the night period and dark grey rectangles represent the subjective
384 day. For each experiment, larvae are entrained for 5 LD cycles the larvae are therefore 5dpf at the
385 beginning of locomotor activity measurements. Locomotor activity is tracked either in constant
386 darkness for 4 days (DD) or tracked in constant darkness for 4 days and subjected to a 2-hours pulse
387 of light during the night of the 2nd day of constant darkness (PD). The phase of locomotor activity is
388 calculated for each larva before and after the timing of the pulse for DD and PS experiments and the
389 △phase (phase after the pulse – phase before the pulse) is calculated.

390 **B)** Average distance moved (mm/min over 10min) of 3 independent PD experiments. Mean ± SE. The
391 △phase of *opn4xa+/+* and *opn4xa-/-* larvae calculated with the FFT-NLLS method is not significantly
392 different. *opn4xa*+/+ and *opn4xa-/-*show similar levels of activity during the light pulse (p=0.56,
393 Mann-Whitney two-tailed test).

394 **C)** Experimental design of phase advance (PA) experiments. The iconography is similar to A). PA-
395 pulsed larvae were subjected to a one-hour pulse of light at CT21.

396 **D)** Average distance moved (mm/min over 10min) of 3 independent PA experiments. Mean ± SE. The
397 △phase of *opn4xa+/+* and *opn4xa-/-* larvae calculated with the FFT-NLLS method is not significantly
398 different (Mann-Whitney two-tailed test).

399

Condition	**Δphase** Mean±S.D (n)	**P value** Mann-Whitney two-tailed test
DD *opn4xa +/+*	1.64±2.92 (39)	
PD-pulsed *opn4xa +/+*	4.73±2.63 (36)	*opn4xa +/+*: PD vs DD: ****
PD-pulsed *opn4xa -/-*	5.23±4.81 (35)	PD *opn4xa -/-* vs *opn4xa* +/+: 0.32
PA-pulsed *opn4xa +/+*	-2.61±4.05 (60)	*opn4xa +/+*: PA vs DD: ****
PA-pulsed *opn4xa-/-*	-2±2.88 (20)	PA *opn4xa -/-* vs *opn4xa +/+:* 0.39

Table 2: Quantification of the phase shifts in *opn4xa*+/+ versus *opn4xa-/-* larvae kept in DD or submitted to a 2 hours pulse of white light at CT16.

As for table 1, the Δphase is the difference between the phase of the two last cycles and the phase of the two first cycles. A Phase shift was observed in DD owing to the period that is close to 25 hours which generates a ~1 hour-shift every cycle. Phases were calculated with the FFT-NLLS method. Upon a pulse of light at CT16 or CT21 a statistical difference was observed between DD and pulsed ctrl larvae (****, $p<0.0001$ using a Mann-Whitney two-tailed test). In both phase delays (PD, pulse of light at CT16) and phase advance paradigms (PA, pulse of light at CT21), no statistical difference between *opn4xa*+/+ and *opn4xa-/-* was observed using a Mann-Whitney two-tailed test. For each type of paradigm (DD, PD and PA) three independent experiments were pooled.

Since neither the absence of RGCs (Fig 2) nor the loss of *opn4xa*-dependent photosensitivity (Fig 6) abolished the capacity of larvae to photoentrain to pulses of light performed in the early or late subjective night, a possible compensation could occur between RGCs and *opn4xa* expressing cells of the pineal gland. To begin addressing this question, we tested photoentrainment properties of *lak-/-; opn4xa-/-* larvae (referred to as 'double'). Compared to *lak* simple mutants, double mutants did not show an attenuated phase shift response to pulses of light at CT16 or CT21 (Fig 7). This suggests that other photosensitive cells mediate photoentrainment in zebrafish.

Finally, *lak* and *lak/opn4xa* double mutant larvae show similar levels of activity during the light pulse both at CT 16 and CT21 (CT16: *lak* : 18.23 ± 8.65 mm/min over 10min (n=27), double: 19.79 ± 12.39 mm/min over 10min (n=27); p=0.94, CT21 : *lak*: 17.46 ± 6.65 mm/min over 10min (n=27), double: 16.8 ± 8.05 mm/min over 10min (n=27), p=0.42, Mann-Whitney two-tailed test). This suggests an absence of redundancy between RGC and *opn4xa* photosensitivity for masking of locomotor activity.

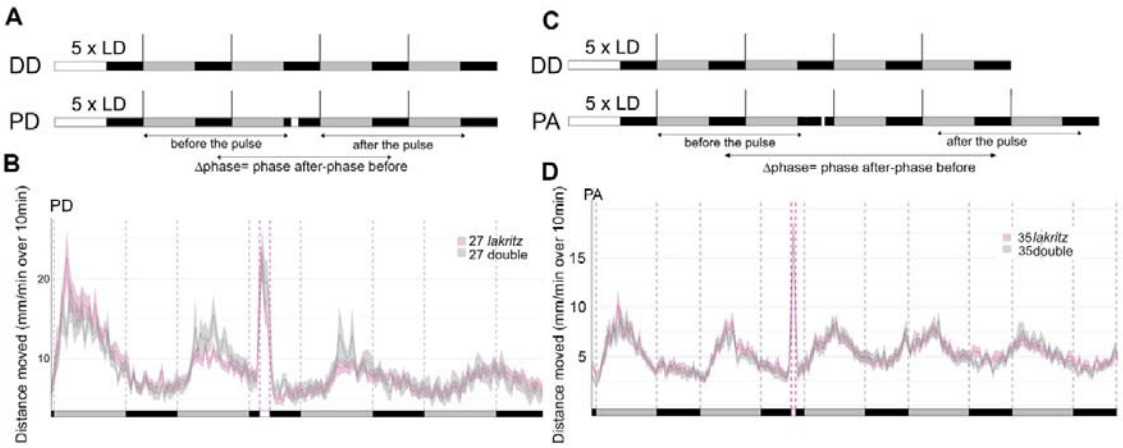

Figure 7: Larvae devoid of RGCs and *opn4xa*-mediated photosensitivity still entrain to pulses of light at CT16 and CT21

A) Experimental design of phase shift experiments. White rectangles represent the day or light pulse period, black rectangles represent the night period and dark grey rectangles represent the subjective day. For each experiment, larvae are entrained for 5 LD cycles the larvae are therefore 5dpf at the beginning of locomotor activity measurements. Locomotor activity is tracked either in constant darkness for 4 days (DD) or tracked in constant darkness for 4 days and subjected to a 2-hours pulse of light during the night of the 2nd day of constant darkness (PD). The phase of locomotor activity is calculated for each larva before and after the timing of the pulse for DD and PS experiments and the △phase (phase after the pulse – phase before the pulse) is calculated.

B) Average distance moved (mm/min over 10min) of 3 independent PD experiments (n=27 for *lak* -/- referred as *lak* and n=27 *lak-/-; opn4xa-/-* larvae referred as 'double'). Mean ± SE. The △phase of *lak* and double larvae calculated with the FFT-NLLS method are not significantly different (see table 3).

C) Experimental design of phase advance (PA) experiments. The iconography is similar to A). After 5 training cycles in LD, PA-pulsed larvae were subjected to a one-hour pulse of light at CT21.

D) Average distance moved (mm/min over 10min) of 3 independent PA experiments (n=27 for *lak* and n=27 double larvae). Error bars represent SE. The △phase of *lak* and double larvae calculated with the FFT-NLLS method are not significantly different (see table 3).

Condition	**Δphase** Mean±S.D (n)	**P value** Mann-Whitney two-tailed test
DD *lak*	2.143 ± 2.09 (31)	
PD-pulsed *lak*	5.72±2.32 (37)	*lak*: PD vs DD: ****
PD-pulsed double	4.90±2.23 (14)	PD double vs *lak*: 0.33
PA-pulsed *lak*	-0.57±4.49(29)	*lak*: PA vs DD:****
PA-pulsed double	-3.16 ± 4.9 (16)	PA double vs *lak* : 0.24

Table 3: Quantification of the phase shifts in *lak* versus double mutant larvae kept in DD or submitted to pulses of white light at CT16 or CT21

As for table 1 and 2, the Δphase is the difference between the phase of the two last cycles and the phase of the two first cycles. A Phase shift is observed in DD owing to the period that is close to 25 hours which generates a ~1 hour-shift every cycle. Phases were calculated with the FFT-NLLS method

450 (biodare2.ed.ac.uk). Upon a pulse of light at CT16 or CT21 a statistical difference is observed
451 between DD and pulsed *lak* larvae (****. p<0.0001 using a Mann-Whitney two-tailed test). In both
452 phase delays (PD, pulse of light at CT16) and phase advance paradigms (PA. pulse of light at CT21), no
453 statistical difference between *lak* and double larvae is observed using a Mann-Whitney two-tailed
454 test. For each type of paradigm DD, PD and PA three independent experiments were pooled.
455
456
457 ## Discussion

458 Experiments performed in mouse have established a role for melanopsin expressing cells of the eye
459 in mediating light input to the circadian rhythm in mammals. In addition to the eye, non-mammalian
460 vertebrates exhibit several extraocular sites of photoreception, raising the question of the relative
461 impact of those different inputs. Herein we show that circadian rhythms of locomotor activity are
462 established and photoentrain in the absence of RGCs in zebrafish larvae. Furthermore, our results
463 show that the absence of a functional eye affects masking, but in a circadian dependent manner. As
464 zebrafish also possesses melanopsin expressing cells in their pineal gland (Sapède et al., 2020), we
465 engineered an *opn4xa* mutant line to address the role of *opn4xa*-dependent photosensitivity in this
466 structure. Our data suggests that *opn4xa* is neither involved in masking nor in the
467 establishment/photoentrainment of circadian rhythms. While our analysis does not support a
468 redundant role for RGCs and *opn4xa* photosensitivity during photoentrainment of circadian
469 rhythms it reveals a subtle function of *opn4xa*-dependent photosensitivity, possibly in the pineal, in
470 the control of period length of circadian rhythms in constant light.

471 **Subtle defects in *opn4xa-/-* mutants in LL**

472 While no differences in period or amplitude of locomotor rhythms are observed for *opn4xa*
473 mutant larvae in DD, subtle alterations are observed in LL. Abrogation of *opn4xa* activity reduces the
474 increase of period length observed when larvae are placed in LL. A similar defect is observed in *Opn4-*
475 */-* mice placed in constant light condition (Panda et al., 2002; Ruby et al., 2002) suggesting this could
476 be a conserved function of melanopsin. Interestingly, this phenotype is not observed in *lak* mutant
477 suggesting that in zebrafish this melanopsin function might involve the pineal gland rather than the
478 eye. While the effect of *opn4xa* mutation on period length in LL is subtle, such an effect is not at all
479 observed in DD. We see two possible hypotheses. First, *opn4xa* homozygous larvae could sense less
480 light than controls and since period shows a reverse correlation with the intensity of light exposure
481 (Aschoff, 1960; Ben-Moshe Livne et al., 2016), it could result in a lower period. A second hypothesis
482 is that the *opn4xa* -/- clock is less stable in LL compared to DD. Indeed, we observed a stronger
483 dampening of the circadian rhythms in LL compared to DD especially when four cycles were filmed
484 and despite a moderate light intensity (20 lux). Along the same line, the variation observed for the

485 periods are higher in LL than in DD for both control and mutant larvae suggesting again less
486 robustness in clock activity in constant light conditions.

487 While we have analysed the expression of clock genes our results did not yield a clear
488 molecular explanation for the *opn4xa* -/- period phenotype in LL. Indeed *opn4xa* -/- larvae only show
489 a modest increase in *Bmal1a*, *cry1* and *dec1* expression in LL (Figure 5). A loss of *dec1* using
490 morpholino antisense technology suggests a role for this gene in controlling circadian rhythms of
491 locomotor activity induced by a light pulse but a role for this gene in period control in LL has not
492 been addressed (Ben-Moshe et al., 2014). Along the same line a double mutant line for *per2* and
493 *cry1a* exhibit deficits in the generation of rhythms following a light pulse but the role of *cry1a* during
494 period control in LL has not been addressed (Hirayama et al., 2019) In contrast, *per2* regulates
495 period length in constant light but its transcription is not affected in *opn4xa-/-* larvae ((Ruggiero et
496 al., 2021; Wang et al., 2015); Figure 5G)); it is however possible that affecting the level of CRY1A
497 could modify PER2 activity therefore leading to the observed phenotype. Further experiments will be
498 required to address this question.

499 **RGCs, but not *opn4xa*, are involved in masking**

500 Compared to their control siblings, we found *lak* mutant larvae to be less active during
501 the light phases of LD cycles as well as when subjected to a pulse of light at CT16 but not at CT21.
502 This reveals a role for RGCs in positive masking in zebrafish larvae as well as a circadian control of this
503 masking activity. It is important to note that while we refer to this as an effect of 'masking' it is at
504 this step impossible to distinguish whether the *lak* mutation impairs the arousing effect of visual
505 stimuli or the arousing effect of light itself. Moreover, masking is not completely abolished
506 in *lak* mutant larvae: in LD as well as during a light pulse at CT16, *lak* mutant larvae still show some
507 masking, albeit at a reduced level and masking is not affected in these larvae at CT21. Could *opn4xa*
508 photosensitivity from the pineal compensate for the lack of RGCs? *opn4xa* -/- larvae display no defect
509 in masking of locomotor activity in LD or during a pulse of light suggesting that *opn4xa*-dependent
510 photosensitivity is dispensable for this type of masking. In addition, *lak*;*opn4xa* double mutants show
511 a similar activity to *lak*-/- larvae during a pulse of light at CT16 and CT21, suggesting that there is no
512 redundancy between the eye and *opn4xa*+ cells in the pineal for masking control. Other
513 photosensitive cells are thus involved in this process. Among these could be the classical
514 photoreceptors of the pineal or deep brain photoreceptors, such as those involved in the
515 locomotor response to a loss of illumination (Fernandes et al., 2012).

516 **A Differential Role for RGCs in controlling phase advance versus phase delays in the**
517 **rhythms of locomotor activity?**

518 *lak* mutant larvae show a reduced phase-advance but no defect in a phase delay paradigm
519 which could indicate a specific role for the RGC in controlling photoentrainment in a phase-advance
520 context. On the other hand, *lak* mutant larvae display less aggregated pigment granules than siblings
521 (Figure S5) Could this impact the way light penetrates their body? While this remains a possibility, we
522 do not think it is a very likely hypothesis since 1.even in *lak* mutant there are rather wide pigment-
523 free areas over the fish brain and in particular over the pineal (Figure S5B) 2.light can still penetrate
524 from the side of the body as pigments are found only on the dorsal and ventral most epidermis
525 (Figure S5C). Finally, experiments aiming at targeting different RGC subpopulations will help
526 consolidate the role of the eye in controlling phase advances as well as identifying downstream
527 circuits.
528
529
530 **RGCs and *opn4xa* are largely dispensable for shifting circadian rhythms of locomotor activity in**
531 **response to a pulse of white light**

532 The present study shows that neither the eye nor *opn4xa* mediated photosensitivity in the
533 pineal gland is absolutely required for the development of circadian rhythms and circadian
534 photoentrainment. The absence of a strong requirement for the eye to control the circadian system
535 in zebrafish is surprising given that *Astyanax mexicanus* blind cavefishes are arrhythmic in DD (Beale
536 et al., 2013) while *Phreatichthys andruzzii* adult cavefishes, which also exhibit a complete eye
537 degeneration, and are arrhythmic in LD when fed at random times (Cavallari et al.. 2011). In light of
538 our data, we propose that apart from the eye, other photosensitive structures might be affected in
539 these other fish species. This in turn brings the question of which structure(s) relay light information
540 to control circadian rhythm in fishes and other non-mammalian animals? The pineal gland, with its
541 classical photoreceptors and *opn4xa*+ projection neurons is an appealing candidate (Sapède and Cau.
542 2013). Strategies aiming at genetically killing this structure or impairing its activity will surely help
543 unravelling its function. Studies describing the effect of surgical pinealectomy have been reported in
544 a number of non-mammalian vertebrates. The phenotypes induced seem to depend strongly on the
545 species. For instance, pinealectomy abolishes rhythms in the stinging catfish but not in the amur
546 catfish or the lake chub. Interestingly, in species where rhythms are maintained upon pinealectomy a
547 change in period can occur (see (Zhdanova and Reebs, 2005) for a review). A similar variety of
548 phenotypes are induced upon pinealectomy in reptiles or birds. In addition to the pineal gland,
549 reptiles have a parietal eye, a structure that is developmentally and spatially related to the pineal
550 gland. Interestingly simultaneous removal of the eye, the pineal gland and the parietal eye in two
551 species of lizards (*P. Sicula* and *S. olivaceous*), does not impair rhythms of locomotor activity while on

552 the contrary these rhythms are lost if in addition to this triple ablation injection of dark ink between
553 the skin and the skull is performed (Tosini et al.. 2001). Similarly, experiments in songbirds suggest
554 the existence of additional photosensitive structures located in the brain that control
555 photoentrainment (Menaker and Underwood. 1976). Altogether these results highlight the existence
556 of other brain structures mediating light inputs on the circadian system. Interestingly, melanopsin
557 expression has been described in other brain areas in the zebrafish larva: *opn4a* is expressed within
558 the presumptive optic area, *opn4b* is found in the ventral forebrain and the thalamic region,
559 and *opn4.1* is detected in a specific domain located in the ventricular region at the junction between
560 the caudal hindbrain and the anterior spinal cord (Fernandes et al.. 2012; Matos-Cruz et al.. 2011).
561 Larvae double mutant for *opn4.1* and *opn4xb* show a decreased locomotor activity during the day
562 but no circadian phenotype (Dekens et al., 2022). As 42 opsin genes are predicted in the zebrafish
563 genome, of which 20 are expressed in the adult brain (Davies et al., 2015), further characterization of
564 their expression in the larval brain will be needed to define the best candidates for further study.
565 Finally, the possibility remains that photoentrainment in zebrafish occurs as a result of direct
566 photosensitivity of motoneurons or muscles themselves as all cells and organs have been shown to
567 be directly photosensitive and light-entrainable in this species (see (Vatine et al., 2011) for a review).
568 Taken together, our results highlight profound differences in the establishment and
569 photoentrainment of the circadian system between the diurnal zebrafish and other species such as
570 mice and human. A crucial, yet open question is whether these divergences reflect the different
571 phylogeny of these species or their different use of temporal niches. The photosensitive capabilities
572 of the zebrafish in particular and of aquatic species in general (as judged by the number of opsins
573 predicted in the genome) far exceed that observed in mammals. This could imply a greater level of
574 complexity and robustness in circadian control in zebrafish independently of its temporal niche.
575 However, the human brain also expresses opsins (*OPN3* and *OPN5*; (Halford et al., 2001; Tarttelin et
576 al., 2003)) suggesting the existence of deep brain photoreceptors in diurnal primates and the
577 possibility that they participate in photoentrainment.

578 **Declaration of competing interest**

579 The authors declare that no competing interests exist.

580 **Acknowledgements**

581 We are indebted to C. Rampon for allowing us to use the Ethovision Software as well as Julie Batut,
582 Ouria Dkhissy Benyahya and Frederique Gaits-Iacovoni for helpful discussions. We thank M. Halpern
583 and K. Soanes for sharing probes. This work was supported by the Centre National de la Recherche
584 Scientifique (CNRS); the Institut National de la Santé et de la Recherche Médicale (INSERM);
585 Université de Toulouse III (UPS); Fondation pour la Recherche Médicale (FRM; DEQ20131029166);
586 Fédération pour la Recherche sur le Cerveau (FRC); Association pour la Recherche sur le Cancer

587 (ARC); Association Rétina France and the Ministère de la Recherche. We would like to thank Brice
588 Ronsin, Stéphanie Bosch and the Toulouse RIO Imaging platform; Stéphane Relexans, Aurore Laire
589 and Richard Brimicombe for taking care of the fish as well as Sophie Polès for technical help.

590 **MATERIAL AND METHODS**

591 **Zebrafish lines and developmental conditions**

592 All animals were handled in the CBI fish facility, which is certified by the French Ministry of
593 Agriculture (approval number A3155510). The project was approved by the French Ministry of
594 Teaching and Research (agreement number APAFIS#3653-2.016.011.512.005.922). Embryos were
595 reared at 28 degrees in a 14h light/10h dark cycle with lights on at 9:00 and lights off at 23:00.
596 The *lak* mutant line has been described previously (Kay et al., 2001), *lak* homozygous mutants were
597 identified by their dark coloration. The protocol for genotyping *lak* individuals is available upon
598 request.
599

600 **Generation of an *opn4xa* mutant allele**

601 An *opn4xa* mutant allele was generated using the CRISPR/ Cas9 targeted genome editing. For this. a
602 target site was designed in the second exon by manual screening for PAM sites. Transcription of the
603 guide and coinjection of the guide mRNA with cas9 mRNA was performed as described in (Lekk et al.,
604 2019). Screening of potential mutants was performed using T7 endonuclease (NEB) treatment of PCR
605 products amplifying the second *opn4xa* exon (Fw : 5' CACAACATAAACTGTAACTGCATCC 3', Rev : 5'
606 GACACGGGTATGACACTCAGGAAGG 3'). PCR products from potential carriers were subsequently
607 subcloned and sequenced. In this manner we identified several interesting carriers among which an
608 individual transmitting an allele bearing 17 extra nucleotides in the second exon leading to a
609 premature interruption of the coding sequence.

610 To genotype *opn4xa* individuals, we used a classical PCR protocol with the following oligos: 5'-
611 GGACGCCTCCAAACTTC-3' (Forward) and 5'-CGAACACCCACTCCTTGTAC-3' Reverse). PCR products of
612 different sizes were obtained (110bp for the wt allele and 127bp for the mutant allele) and resolved
613 on a 4% agarose gel.
614

615 **Locomotor Activity Assays**

616 Larvae zebrafish coming from heterozygous incrosses were raised on a 14:10 hr light:dark cycle at
617 28°C in Petri dishes with no more than 50 larvae per Petri dish in a water bath inside the fish facility.
618 On the morning of their 5th day of development (9:15-10:30), individual larvae were placed in each
619 well of a 96-well plate containing aquarium fish water and placed back in the water bath. Light
620 intensity during the entrainment was 110 lux at 6500K. On the evening (16:00-20:00), the plate was

621 put in an hermetic box in a dark room maintained at 27°C with a heater. This home-made box (Vignet
622 et al., 2013) was continuously illuminated from below with two panels of infra-red lights as well as
623 neutral white light (4000K, 20 lux at water surface)) controlled by a timer from 9:00 to 23:00. Larvae
624 were then filmed at 30 frames per second, with a ceiling mounted infra-red camera connected to a
625 computer on the following days (from the 6th day of development to the 9th or 10th day of
626 development) in controlled conditions of illumination. The temperature inside the box was
627 monitored using an electronic programmable device (I Button. Maxim). After the experiment, larvae
628 were either genotyped by PCR for *opn4xa* and/or *lak* and/or simply identified for the *lak* mutation
629 using the dark coloration phenotype. In addition, larvae presenting developmental defects were
630 discarded from the subsequent analysis. Experiments in which too many larvae presented
631 development issues or where temperature issues were present were discarded. At least three
632 experiments were made for each type of assay.
633
634 **In Situ Hybridization**
635 In situ hybridization was performed as described previously (Cau et al., 2008). *opn4xa, tcf7* and *c-fos*
636 probes have been described previously (Matos-Cruz et al.,2011; Ellis et al.,2012; Sapède et al., 2020).
637
638 **Locomotor Activity Analysis**
639 After the experiment, the distance travelled per minute was extracted for each larva using the
640 Ethovision XT13.0 (Noldus. Wageningen. the Netherlands) with the following parameters: for
641 Detection Settings: dynamic substraction ; subject color compared to background : Darker ; Dark : 7
642 to 210 ; Frame Weight : 2 ; for Track Smoothing Profiles :Minimal Distance Moved : 0.2mm - Direct
643 (A>MDM) ; for Data Profiles : Results per time bin. Ignore last time bin if incomplete; for Analysis
644 Profiles: Distance moved of the center-point. The obtained files were then analysed using the
645 wakefish program (written in python by L.Sanchou) to extract an average activity of mm/min over
646 10min for each larva ('DM10 files'). For each experiment, the same number of homozygous mutants
647 and wild-type or control larvae were randomly selected. The Biodare software was used to calculate
648 periods and phases for each larva (biodare2.ed.ac.uk). We choose to use the FFT-NLLS to calculate
649 periods and phases on DM10 files after baseline detrending, as advised (Zielinski et al., 2014). The
650 parameters used for period calculation were as follows: baseline detrending, expected periods from
651 18 to 30 hours. analysis method FFT-NLLS. The parameters used for phase calculation were as
652 follows: baseline detrending. FFT-NLLS, phase by fit, absolute phase to window. Windows used to
653 calculate the phase of locomotor activity "before the pulse" and "after the pulse" encompass time
654 points from CT0 to CT15 (corresponding from 9am of the 1st day in of the experiment to midnight

655 between the 2nd and 3rd day of the experiment for "before the pulse" and from 9am of the 3rd day of
656 the experiment to midnight between the 4th and 5th day of the experiment). Locomotor activity levels
657 were calculated from the DM10 files by calculating means of the average activity in mm/min over 10
658 min over a given period for each larva. Statistical analysis was done using Prism. Graphs were
659 generated using R studio (ggplot2 and rethomics packages (Geissmann et al., 2019; Wickham, 2016)).
660

661 **Analysis of clock gene expression using RTqPCR :**

662 For each specific stage, pools of 15 larvae were collected and extracted with TRIzol. Reverse
663 transcription and qPCR were performed using a standard protocol (Quillien et al., 2021) with the
664 oligos detailed in Supplemental Table 7. All the experiments were performed in triplicates and the
665 mean expression relative to beta actin was calculated .Three pools of larvae were used for each time
666 point.

667 **REFERENCES**

668 **Altimus, C. M., Güler, A. D., Villa, K. L., McNeill, D. S., Legates, T. A. and Hattar, S.** (2008). Rods-
669 cones and melanopsin detect light and dark to modulate sleep independent of image
670 formation. *Proc. Natl. Acad. Sci. U. S. A.* **105**, 19998–20003.

671 **Aschoff, J.** (1960). Exogenous and endogenous components in circadian rhythms. *Cold Spring Harb.*
672 *Symp. Quant. Biol.* **25**, 11–28.

673 **Baver, S. B., Pickard, G. E., Sollars, P. J. and Pickard, G. E.** (2008). Two types of melanopsin retinal
674 ganglion cell differentially innervate the hypothalamic suprachiasmatic nucleus and the
675 olivary pretectal nucleus. *Eur. J. Neurosci.* **27**, 1763–1770.

676 **Beale, A., Guibal, C., Tamai, T. K., Klotz, L., Cowen, S., Peyric, E., Reynoso, V. H., Yamamoto, Y. and**
677 **Whitmore, D.** (2013). Circadian rhythms in Mexican blind cavefish Astyanax mexicanus in the
678 lab and in the field. *Nat. Commun.* **4**, 1–10.

679 **Belenky, M. A., Smeraski, C. A., Provencio, I., Sollars, P. J. and Pickard, G. E.** (2003). Melanopsin
680 retinal ganglion cells receive bipolar and amacrine cell synapses. *J. Comp. Neurol.* **460**, 380–
681 393.

682 **Ben-Moshe, Z., Alon, S., Mracek, P., Faigenbloom, L., Tovin, A., Vatine, G. D., Eisenberg, E., Foulkes,**
683 **N. S. and Gothilf, Y.** (2014). The light-induced transcriptome of the zebrafish pineal gland
684 reveals complex regulation of the circadian clockwork by light. *Nucleic Acids Res.* **42**, 3750–
685 3767.

686 **Ben-Moshe Livne, Z., Alon, S., Vallone, D., Bayleyen, Y., Tovin, A., Shainer, I., Nisembaum, L. G.,**
687 **Aviram, I., Smadja-Storz, S., Fuentes, M., et al.** (2016). Genetically Blocking the Zebrafish
688 Pineal Clock Affects Circadian Behavior. *PLoS Genet.* **12**, e1006445.

689 **Bhadra, B., N, T., P, D. and M, P. B.** (2017). Evolution of circadian rhythms: from bacteria to human.
690 *Sleep Med.*

691 **Brzezinski, J. A., Brown, N. L., Tanikawa, A., Bush, R. A., Sieving, P. A., Vitaterna, M. H., Takahashi,**
692 **J. S. and Glaser, T.** (2005). Loss of Circadian Photoentrainment and Abnormal Retinal
693 Electrophysiology in Math5 Mutant Mice. *Invest. Ophthalmol. Vis. Sci.* **46**, 2540–2551.

694 **Calligaro, H., Coutanson, C., Najjar, R. P., Mazzaro, N., Cooper, H. M., Haddjeri, N., Felder-**
695 **Schmittbuhl, M.-P. and Dkhissi-Benyahya, O.** (2019). Rods contribute to the light-induced
696 phase shift of the retinal clock in mammals. *PLoS Biol.* **17**, e2006211.

697 **Carr, A.-J. F. and Whitmore, D.** (2005). Imaging of single light-responsive clock cells reveals
698 fluctuating free-running periods. *Nat. Cell Biol.* **7**, 319–321.

699 **Cau, E., Quillien, A. and Blader, P.** (2008). Notch resolves mixed neural identities in the zebrafish
700 epiphysis. *Dev. Camb. Engl.* **135**, 2391–2401.

701 **Cavallari, N., Frigato, E., Vallone, D., Fröhlich, N., Lopez-Olmeda, J. F., Foà, A., Berti, R., Sánchez-**
702 **Vázquez, F. J., Bertolucci, C. and Foulkes, N. S.** (2011). A Blind Circadian Clock in Cavefish
703 Reveals that Opsins Mediate Peripheral Clock Photoreception. *PLoS Biol.* **9**,.

704 **Chew, K. S., Renna, J. M., McNeill, D. S., Fernandez, D. C., Keenan, W. T., Thomsen, M. B., Ecker, J.**
705 **L., Loevinsohn, G. S., VanDunk, C., Vicarel, D. C., et al.** (2017). A subset of ipRGCs regulates
706 both maturation of the circadian clock and segregation of retinogeniculate projections in
707 mice. *eLife* **6**, e22861.

708 **Covello, G., Rossello, F. J., Filosi, M., Gajardo, F., Duchemin, A., Tremonti, B. F., Eichenlaub, M.,**
709 **Polo, J. M., Powell, D., Ngai, J., et al.** (2020). Transcriptome analysis of the zebrafish
710 atoh7−/− Mutant, lakritz, highlights Atoh7-dependent genetic networks with potential
711 implications for human eye diseases. *FASEB BioAdvances* **2**, 434–448.

712 **Davies, W. I. L., Tamai, T. K., Zheng, L., Fu, J. K., Rihel, J., Foster, R. G., Whitmore, D. and Hankins,**
713 **M. W.** (2015). An extended family of novel vertebrate photopigments is widely expressed
714 and displays a diversity of function. *Genome Res.* **25**, 1666–1679.

715 **Dekens, M. P. S., Fontinha, B. M., Gallach, M., Pflügler, S. and Tessmar-Raible, K.** (2022).
716 Melanopsin elevates locomotor activity during the wake state of the diurnal zebrafish. *EMBO*
717 *Rep.* **23**, e51528.

718 **Dkhissi-Benyahya, O., Gronfier, C., De Vanssay, W., Flamant, F. and Cooper, H. M.** (2007). Modeling
719 the role of mid-wavelength cones in circadian responses to light. *Neuron* **53**, 677–687.

720 **Dollet, A., Albrecht, U., Cooper, H. M. and Dkhissi-Benyahya, O.** (2010). Cones Are Required for
721 Normal Temporal Responses to Light of Phase Shifts and Clock Gene Expression. *Chronobiol.*
722 *Int.* **27**, 768–781.

723 **Fernandes, A. M., Fero, K., Arrenberg, A. B., Bergeron, S. A., Driever, W. and Burgess, H. A.** (2012).
724 Deep brain photoreceptors control light seeking behavior in zebrafish larvae. *Curr. Biol. CB*
725 **22**, 2042–2047.

726 **Fernandez, D. C., Chang, Y.-T., Hattar, S. and Chen, S.-K.** (2016). Architecture of retinal projections to
727 the central circadian pacemaker. *Proc. Natl. Acad. Sci.* **113**, 6047–6052.

728 **Freedman, M. S., Lucas, R. J., Soni, B., Schantz, M. von, Muñoz, M., David-Gray, Z. and Foster, R.**
729 (1999). Regulation of Mammalian Circadian Behavior by Non-rod, Non-cone, Ocular
730 Photoreceptors. *Science*.

731 **Geissmann, Q., Rodriguez, L. G., Beckwith, E. J. and Gilestro, G. F.** (2019). Rethomics: An R
732 framework to analyse high-throughput behavioural data. *PLOS ONE* **14**, e0209331.

733 **Gompf, H. S., Fuller, P. M., Hattar, S., Saper, C. B. and Lu, J.** (2015). Impaired circadian
734 photosensitivity in mice lacking glutamate transmission from retinal melanopsin cells. *J. Biol.*
735 *Rhythms* **30**, 35–41.

736 **Güler, A. D., Ecker, J. L., Lall, G. S., Haq, S., Altimus, C. M., Liao, H.-W., Barnard, A. R., Cahill, H.,**
737 **Badea, T. C., Zhao, H., et al.** (2008). Melanopsin cells are the principal conduits for rod-cone
738 input to non-image-forming vision. *Nature* **453**, 102–105.

739 **Halford, S., Freedman, Melanie S., Bellingham, J., Inglis, S. L., Poopalasundaram, S., Soni, B. G.,**
740 **Foster, R. G. and Hunt, D. M.** (2001). Characterization of a Novel Human Opsin Gene with
741 Wide Tissue Expression and Identification of Embedded and Flanking Genes on Chromosome
742 1q43. *Genomics* **72**, 203–208.

743 **Hartley, S., Dauvilliers, Y. and Quera-Salva, M.-A.** (2018). Circadian Rhythm Disturbances in the
744 Blind. *Curr. Neurol. Neurosci. Rep.* **18**, 65.

745 **Hirayama, J., Alifu, Y., Hamabe, R., Yamaguchi, S., Tomita, J., Maruyama, Y., Asaoka, Y., Nakahama,**
746 **K.-I., Tamaru, T., Takamatsu, K., et al.** (2019). The clock components Period2,
747 Cryptochrome1a, and Cryptochrome2a function in establishing light-dependent behavioral
748 rhythms and/or total activity levels in zebrafish. *Sci. Rep.* **9**, 196.

749 **Karnas, D., Hicks, D., Mordel, J., Pévet, P. and Meissl, H.** (2013). Intrinsic Photosensitive Retinal
750 Ganglion Cells in the Diurnal Rodent, Arvicanthis ansorgei. *PLOS ONE* **8**, e73343.

751 **Kay, J. N., Finger-Baier, K. C., Roeser, T., Staub, W. and Baier, H.** (2001). Retinal Ganglion Cell
752 Genesis Requires lakritz, a Zebrafish atonal Homolog. *Neuron* **30**, 725–736.

753 **Kofuji, P., Mure, L. S., Massman, L. J., Purrier, N., Panda, S. and Engeland, W. C.** (2016). Intrinsically
754 Photosensitive Retinal Ganglion Cells (ipRGCs) Are Necessary for Light Entrainment of
755 Peripheral Clocks. *PLOS ONE* **11**, e0168651.

756 **Kölsch, Y., Hahn, J., Sappington, A., Stemmer, M., Fernandes, A. M., Helmbrecht, T. O., Lele, S.,**
757 **Butrus, S., Laurell, E., Arnold-Ammer, I., et al.** (2021). Molecular classification of zebrafish
758 retinal ganglion cells links genes to cell types to behavior. *Neuron* **109**, 645-662.e9.

759 **Lekk, I., Duboc, V., Faro, A., Nicolaou, S., Blader, P. and Wilson, S. W.** (2019). Sox1a mediates the
760 ability of the parapineal to impart habenular left-right asymmetry. *eLife* **8**, e47376.

761 **Li, J. Y. and Schmidt, T. M.** (2018). Divergent projection patterns of M1 ipRGC subtypes. *J. Comp.*
762 *Neurol.* **526**, 2010–2018.

763 **Lockley, S. W., Arendt, J. and Skene, D. J.** (2007). Visual impairment and circadian rhythm disorders.
764 *Dialogues Clin. Neurosci.* **9**, 301–314.

765 **Masai, I., Stemple, D. L., Okamoto, H. and Wilson, S. W.** (2000). Midline Signals Regulate Retinal
766 Neurogenesis in Zebrafish. *Neuron* **27**, 251–263.

767 **Matos-Cruz, V., Blasic, J., Nickle, B., Robinson, P. R., Hattar, S. and Halpern, M. E.** (2011).
768 Unexpected diversity and photoperiod dependence of the zebrafish melanopsin system. *PloS*
769 *One* **6**, e25111.

770 **Menaker, M. and Underwood, H.** (1976). Extraretinal Photoreception in Birds. *Photochem.*
771 *Photobiol.* **23**, 299–306.

772 **Mure, L. S.** (2021). Intrinsically Photosensitive Retinal Ganglion Cells of the Human Retina. *Front.*
773 *Neurol.* **12**, 636330.

774 **Neuhauss, S. C. F., Biehlmaier, O., Seeliger, M. W., Das, T., Kohler, K., Harris, W. A. and Baier, H.**
775 (1999). Genetic Disorders of Vision Revealed by a Behavioral Screen of 400 Essential Loci in
776 Zebrafish. *J. Neurosci.* **19**, 8603–8615.

777 **Panda, S., Sato, T. K., Castrucci, A. M., Rollag, M. D., DeGrip, W. J., Hogenesch, J. B., Provencio, I.**
778 **and Kay, S. A.** (2002). Melanopsin (Opn4) requirement for normal light-induced circadian
779 phase shifting. *Science* **298**, 2213–2216.

780 **Perez-Leon, J. A., Warren, E. J., Allen, C. N., Robinson, D. W. and Brown, R. L.** (2006). Synaptic inputs
781 to retinal ganglion cells that set the circadian clock. *Eur. J. Neurosci.* **24**, 1117–1123.

782 **Quillien, A., Gilbert, G., Boulet, M., Ethuin, S., Waltzer, L. and Vandel, L.** (2021). Prmt5 promotes
783 vascular morphogenesis independently of its methyltransferase activity. *PLoS Genet.* **17**,.

784 **Ruby, N. F., Brennan, T. J., Xie, X., Cao, V., Franken, P., Heller, H. C. and O'Hara, B. F.** (2002). Role of
785 melanopsin in circadian responses to light. *Science* **298**, 2211–2213.

786 **Ruggiero, G., Ben-Moshe Livne, Z., Wexler, Y., Geyer, N., Vallone, D., Gothilf, Y. and Foulkes, N. S.**
787 (2021). Period 2: A Regulator of Multiple Tissue-Specific Circadian Functions. *Front. Mol.*
788 *Neurosci.* **14**, 718387.

789 **Rupp, A. C., Ren, M., Altimus, C. M., Fernandez, D. C., Richardson, M., Turek, F., Hattar, S. and**
790 **Schmidt, T. M.** (2019). Distinct ipRGC subpopulations mediate light's acute and circadian
791 effects on body temperature and sleep. *eLife* **8**, e44358.

792 **Sack, R. L., Lewy, A. J., Blood, M. L., Keith, L. D. and Nakagawa, H.** (1992). Circadian rhythm
793 abnormalities in totally blind people: incidence and clinical significance. *J. Clin. Endocrinol.*
794 *Metab.* **75**, 127–134.

795 **Sapède, D. and Cau, E.** (2013). The pineal gland from development to function. *Curr. Top. Dev. Biol.*
796 **106**, 171–215.

797 **Sapède, D., Chaigne, C., Blader, P. and Cau, E.** (2020). Functional heterogeneity in the pineal
798 projection neurons of zebrafish. *Mol. Cell. Neurosci.* **103**, 103468.

799 **Tamai, T. K., Young, L. C. and Whitmore, D.** (2007). Light signaling to the zebrafish circadian clock by
800 Cryptochrome 1a. *Proc. Natl. Acad. Sci. U. S. A.* **104**, 14712–14717.

801 **Tarttelin, E. E., Bellingham, J., Hankins, M. W., Foster, R. G. and Lucas, R. J.** (2003). Neuropsin
802 (Opn5): a novel opsin identified in mammalian neural tissue 1. *FEBS Lett.* **554**, 410–416.

803 **Tosini, G., Bertolucci, C. and Foà, A.** (2001). The circadian system of reptiles: a multioscillatory and
804 multiphotoreceptive system. *Physiol. Behav.* **72**, 461–471.

805 **Vallone, D., Gondi, S. B., Whitmore, D. and Foulkes, N. S.** (2004). E-box function in a period gene
806 repressed by light. *Proc. Natl. Acad. Sci. U. S. A.* **101**, 4106–4111.

807 **Vatine, G., Vallone, D., Gothilf, Y. and Foulkes, N. S.** (2011). It's time to swim! Zebrafish and the
808 circadian clock. *FEBS Lett.* **585**, 1485–1494.

809 **Wang, M., Zhong, Z., Zhong, Y., Zhang, W. and Wang, H.** (2015). The Zebrafish Period2 Protein
810 Positively Regulates the Circadian Clock through Mediation of Retinoic Acid Receptor (RAR)-
811 related Orphan Receptor α (Rorα). *J. Biol. Chem.* **290**, 4367–4382.

812 **Wee, R., Castrucci, A. M., Provencio, I., Gan, L. and Van Gelder, R. N.** (2002). Loss of Photic
813 Entrainment and Altered Free-Running Circadian Rhythms in math5−/− Mice. *J. Neurosci.* **22**,
814 10427–10433.

815 **Whitmore, D., Foulkes, N. S. and Sassone-Corsi, P.** (2000). Light acts directly on organs and cells in
816 culture to set the vertebrate circadian clock. *Nature* **404**, 87–91.

817 **Wickham, H.** (2016). ggplot2: Elegant Graphics for Data Analysis. *Springer-Verl. N. Y. ISBN 978-3-319-*
818 *24277-4*.

819 **Wong, K. Y., Dunn, F. A., Graham, D. M. and Berson, D. M.** (2007). Synaptic influences on rat
820 ganglion-cell photoreceptors. *J. Physiol.* **582**, 279–296.

821 **Zhdanova, I. V. and Reebs, S. G.** (2005). Circadian Rhythms in Fish. *Fish Physiol. Acad. Press* 197–238.

822 **Zielinski, T., Moore, A. M., Troup, E., Halliday, K. J. and Millar, A. J.** (2014). Strengths and Limitations
823 of Period Estimation Methods for Circadian Data. *PLOS ONE* **9**, e96462.

824

825 **<u>Supplemental data:</u>**

826

827 **Supplemental Figure 1:**

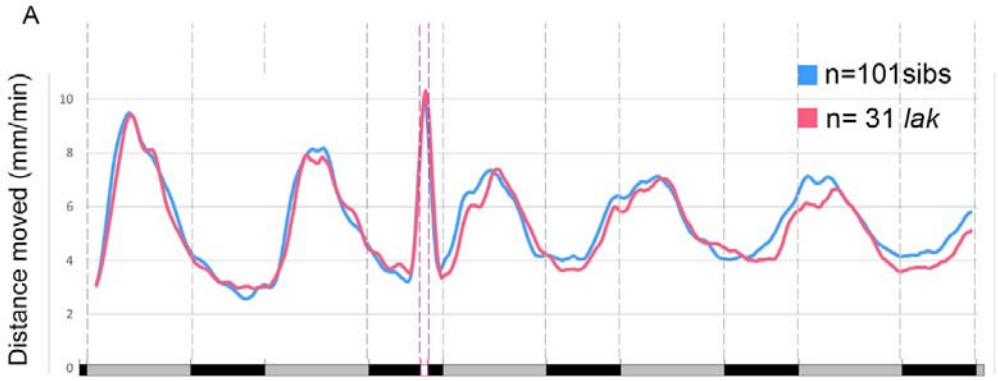

828

829 Figure S1 : (A) Average distance moved merged from PA experiments in 10 min bins. Mean ± SE. The
830 original data is the same than in figure2 but here, only the larvae for which a phase could be
831 extracted for the two first and the two last cycles were included in the average. In addition, two
832 rounds of smoothing each using ten successive time points were applied as this made the difference
833 in phase shift between the *lak* and the sib larvae more easy to visualize.

834

835 **Supplemental Figure 2 :**

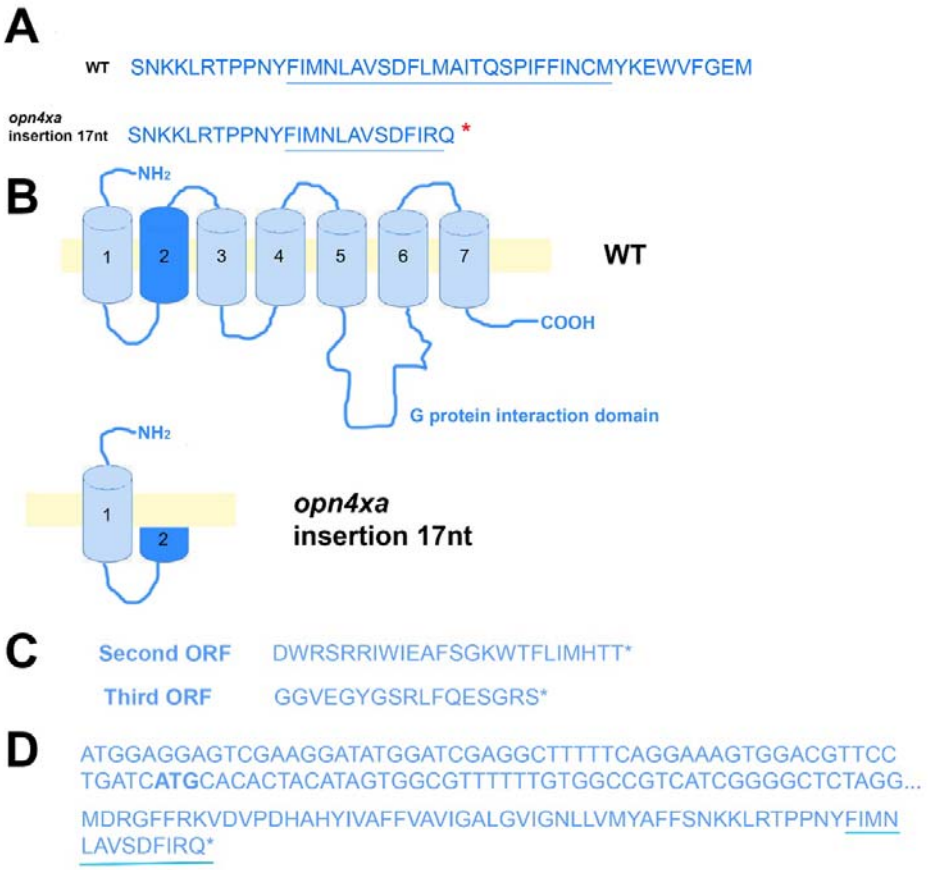

A)Prediction of the protein sequences produced by the wt and mutant exon 2. The part corresponding to the second transmembrane domain (Matos-Cruz et al., 2011) is underlined. The red asterisk indicates a premature stop codon. (B) Models of the WT and mutant predicted OPN4XA proteins.(C) Predicted proteins produced from alternative codon usage of the mutant cDNA. (D) cDNA sequence of the beginning of the *opn4xa* gene, a secondary ATG is indicated in bold. Below, the predicted protein produced from this alternative ATG in the mutant cDNA is indicated. In all cases described in C and D, the predicted mutant protein is truncated.

Supplemental Figure 3:

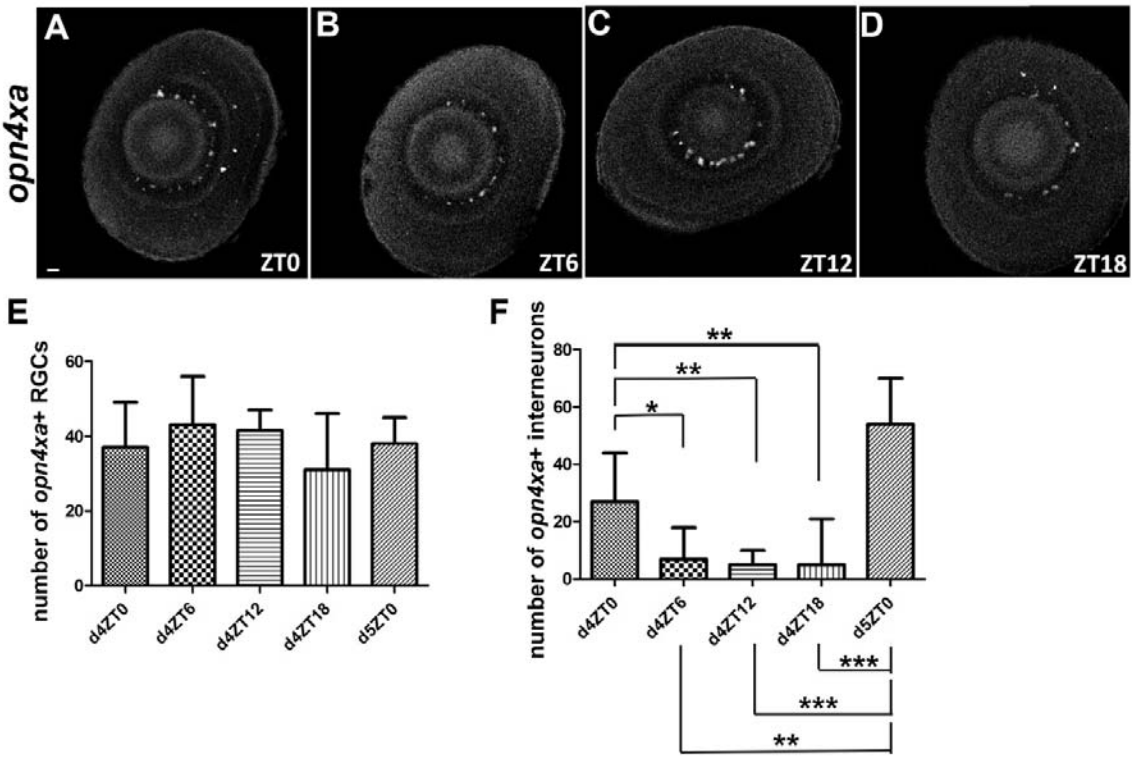

Figure S3: *opn4xa* is expressed in zebrafish RGCs and interneurons

(A-D) Expression of *opn4xa* at 4days at different ZT using fluorescent in situ hybridization. Lateral view of mounted eyes imaged under the confocal microscope. The ventral side is oriented towards the left upper corner. Based on position, the *opn4xa*+ cells from the interneuron layer are most likely horizontal and amacrine cells. **Scale bar: 10 µm.**

E) Number of *opn4xa*+ cells in the RGC layer in 96-128 hpf zebrafish larvae. All data follows a Gaussian distribution. No statistical differences were observed between the different time points using a one-way ANOVA with Bonferroni post hoc test.

F) Number of *opn4xa*+ cells in the interneuron layer in 96-128 hpf zebrafish larvae. The data at 4dZT0 does not follow a Gaussian distribution. * $p<0.05$. ** $p<0.001$. *** $p<0.0005$ using a Kruskal-Wallis test with Dunn's post hoc comparison.

<u>Supplemental Figure 4:</u>

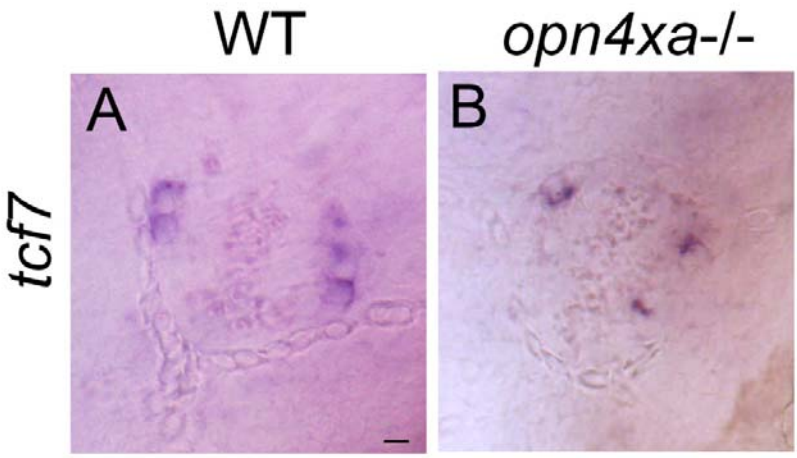

Figure S4: Expression of *tcf7* in the pineal gland at 6 days using in situ hybridization in wt and *opn4xa-/-* larvae. Dorsal views are shown. Scale bar : 10 µm.

Supplemental Figure 5:

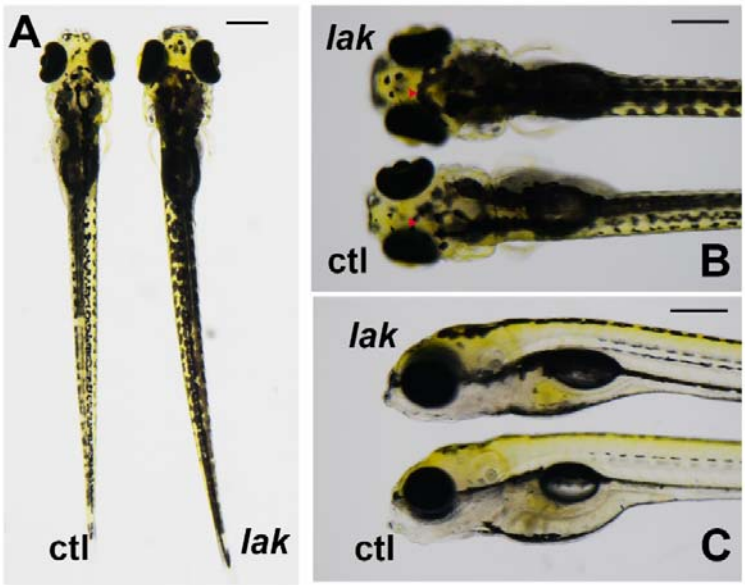

Figure S5 Live *lak* and sibling larvae at 5 dpf showing the differences in pigmentation. A-B) Dorsal views C) side views. The red arrow in B points to the position of the pineal gland which is not covered by pigments in *lak* and sib larvae. Scale bar: 0.5 mm.

Legend for the following supplemental tables:

Legend for the supplemental tables S1-S6

Tables showing the average distance travelled (mm/min) over a 10 min window averaged during the day (D) or the night (N) periods. Mean ± S.D. D1 corresponds to the first day. The p value and statistical significance using a two-tailed Mann-Whitney test is indicated.

Legend for the Supplemental table S7:

List of primers for RTqPCR. The gene ID corresponds to the ZDB number.

Supplemental table 1: activity of *lakritz* -/- versus control larvae in LD

condition	ctrl (n=55)	*lakritz* (n=55)	p value
D1	13.95 ± 9.76	9.72 ± 8.73	**** 0.008**
N1	2.92 ± 2.28	2.85 ± 2.57	n.s 0.42
D2	16.90 ± 10.25	11.18 ± 7.40	***** 0.0005**
N2	4.04 ± 2.22	4.98 ± 4.22	n.s 0.51
D3	13.19 ± 8.56	10.88 ± 7.07	n.s 0.13
N3	3.56 ± 2.17	3.95 ± 2.94	n.s 0.57

Supplemental table 2: activity of *lakritz* -/- versus control larvae in DD

condition	ctrl (n=84)	*lakritz* (n=84)	p value
D1	8.9 ± 8.7	8.73 ± 7.08	n.s 0.43
N1	2.78± 3.4	2.45 ± 1.67	n.s 0.98
D2	6.20 ± 4.18	6.39 ± 5.77	n.s 0.44
N2	2.64 ± 1.60	2.80 ± 5.64	n.s 0.92
D3	6.76 ± 7.25	6.86 ± 5.64	n.s 0.95
N3	3.13 ± 1.95	3.27± 2.16	n.s 0.87
D4	8.68 ± 8.41	8.52 ± 6.89	n.s 0.55
N4	3.42 ± 2.20	3.43 ± 2.18	n.s 0.92

Supplemental table 3: activity of *lakritz* -/- versus control larvae in LL

condition	ctrl (n=72)	*lakritz* (n=72)	p value
D1	21.31±13.33	19.49±12.39	n.s 0.44
N1	7.38±4.59	6.61±4.83	n.s 0.27
D2	22.99±14.01	22.88±19.03	n.s 0.27
N2	8.03±4.35	9.28±6.59	n.s 0.35
D3	17.71±8.51	17.43±14.59	n.s 0.096
N3	8.11±3.63	8.54±5.38	n.s 0.85

Supplemental table 4: activity of *opn4xa* -/- versus control larvae in LD

condition	wt (n=48)	*opn4xa-/-* (n=48)	p value
D1	22.16 ± 10.02	22.42 ± 13.12	n.s 0.73
N1	9.41 ± 6.45	7.94 ± 4.99	n.s 0.30
D2	20.46 ± 7.96	19.49 ± 8.25	n.s 0.50
N2	7.27 ± 4.86	6.32 ± 4.53	n.s 0.27
D3	14.35 ± 5.19	12.52 ± 6.12	n.s 0.07
N3	5.59 ± 3.41	4.19 ± 3.09	*** 0.01**

Supplemental table 5: activity of *opn4xa* -/- versus control larvae in DD

condition	wt (n=65)	*opn4xa-/-* (n=65)	p value
D1	14.73 ± 7.04	16.26 ± 10.22	n.s 0.41
N1	6.54 ± 1.96	6.15 ± 2.27	n.s 0.35

D2	12.52 ± 5.10	13.23 ± 6.58	n.s 0.32
N2	5.62 ± 2.06	6.04 ± 2.59	n.s 0.38
D3	8.94 ± 2.24	9.09 ± 2.93	n.s 0.58
N3	5.49 ± 2.09	5.45 ± 2.21	n.s 0.63
D4	7.15 ± 2.35	7.34 ± 2.33	n.s 0.69
N4	5.13 ± 2.43	5.30 ± 2.01	n.s 0.65

Supplemental table 6: activity of *opn4xa* -/- versus control larvae in LL

condition	wt (n=66)	*opn4xa-/-* (n=66)	p value
D1	16.56 ± 9.57	20.15 ± 12.25	n.s 0.07
N1	3.84 ± 2.99	6.22 ± 5.60	*** 0.02**
D2	16.67 ± 7.79	19.22 ± 11.49	n.s 0.26
N2	4.90 ± 3.30	5.92 ± 4.48	n.s 0.36
D3	14.27 ± 7.16	13.94 ± 7.26	n.s 0.82
N3	5.92 ± 4.09	5.63 ± 3.75	n.s 0.70

Supplemental table 7: qRTPCR primer sequences

Gene	Forward primer	Reverse primer	Gene ID
bmal1a	5'TGTAACGCAATGTCTCGCAAG3'	5'GTGGCCCCTCGTAATGTCTTC3'	000509-1
cry1a	5'AGGCGTGGAGGTGATAGTTC3'	5'TGCTGA'TGAGGGTCTGGAAG3'	010426-2
dec1	5'CGCTGGATATCTCTGACATGCAAGG3'	5'CGTGAGTTTAAGGTGTTCGGGCAG3'	030131-3133
tefa	5'AACCCCTCCACCGAATCTTC3'	5'TCCCATTTCACTGACCCCTC3'	990415-264
per1a	5'GAGACGACGGAAAGCAAGAG3'	5'GCTCTGAACTTCCGCTCAAA3'	011220-1
per1b	5'ATGTGCAGGCTGTAGATCCC3'	5'CCGTCAGTTTCGCTTTTCTC3'	040419-1
reverbB1	5'AGGACGCCATCAGTGTGTTT 3'	5'CTGGCCCAGGAAAACAAGTA3'	040504-1
per2	5'GCTTCACCACACCATACAGG 3'	5'GTCTGACGGGGACGAGTCT3'	011220-2
β-actin	5'GCCTGACGGACAGGTCAT 3'	5' ACCGCAAGATTCCATACCC 3'	000329-1